Downslope Windstorms and Rotors

Jonathan Vigh

AT707

21,23,25 February 2005

Aspects of flow over barriers

- 2D mountain waves
- Flow over/around isolated hills
- Blocking by large amplitude mountains
  - Gap flows, funneling
  - Cold air damming, barrier jets
- Föhn and Bora winds
- Downslope windstorms
- Thermally-driven circulations (slope winds, mountain winds, valley winds), katabatic winds
- Orographic control of precipitation
- Quasi-geostrophic flow over a mountain
- Lee cyclogenesis
- Gravity wave drag

Naming conventions and terminology

What are the different types of downslope winds and where do they occur?

Föhn winds (warming winds)

Föhn (Alps), *Chinook* (Rockies), *zonda* (eastern Andes), *pulche* (western Andes), *Santa Ana* (southern California), *sundowner* (Santa Barbara, CA), *berg* (South Africa), *koschava* and *ljuka (Croatia*), *germich* (SW Caspian Sea), *afganet* and *ibe* (Central Asia), *kachchan* (Sri Lanka), *Canterbury north-wester* (New Zealand)

Bora winds (cooling winds)

bora (Croatia), *mistral* (France)

Glenn (1961) concluded that there was no satisfactory definition for a Föhn flow

- Yoshino (1975) said that the definition should simply be based on whether the temperature of the downslope flowing air was warmer or cooler than the air it was displacing
- Chinooks and boras do not always have severe winds

It is best to just call this phenomenon “downslope windstorm” or “severe downslope windstorm”

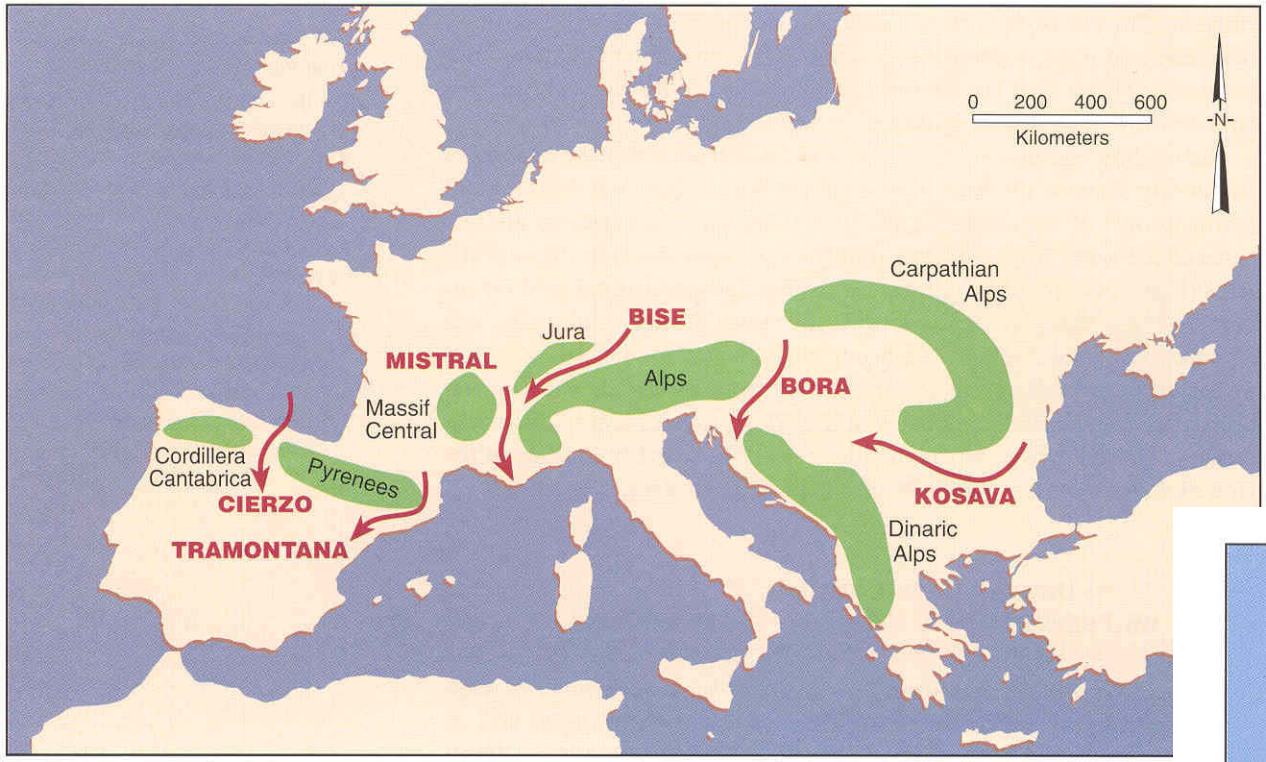

Föhn and bora winds of the Western U.S.

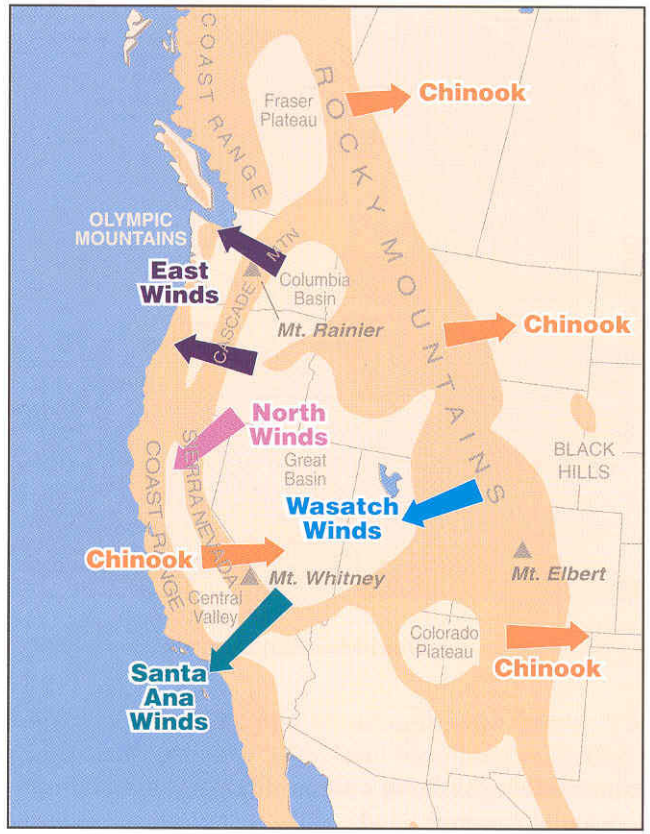

Gap flows between mountains of Europe

Figures from Whiteman (2000)

A few notes on the Chinook

Why are Chinooks warm?

The descending air can be warmer for one or more reasons:

- Compressional heating as air descends the lee side of the mountain (air warms according to the dry adiabatic lapse rate: 9.8 °C per km of descent)
- Latent heat of condensation (Hahn effect): air ascends moist adiabatically (cooling ~5°C per km) on windward side of mountain while precipitation is produced, then descends dry adiabatically on the leeward side
- Blocking on the windward side of the mountain can cause air to descend from a higher level (higher θ)
- Displacement of cold air by warmer air
- Nighttime mixing

Other peculiarities can occur if a cold pool is present

– Waves can propagate on the inversion surface (see Black Hills paper)

– Mirages can make the mountains look higher

Figures from Whiteman (2000)

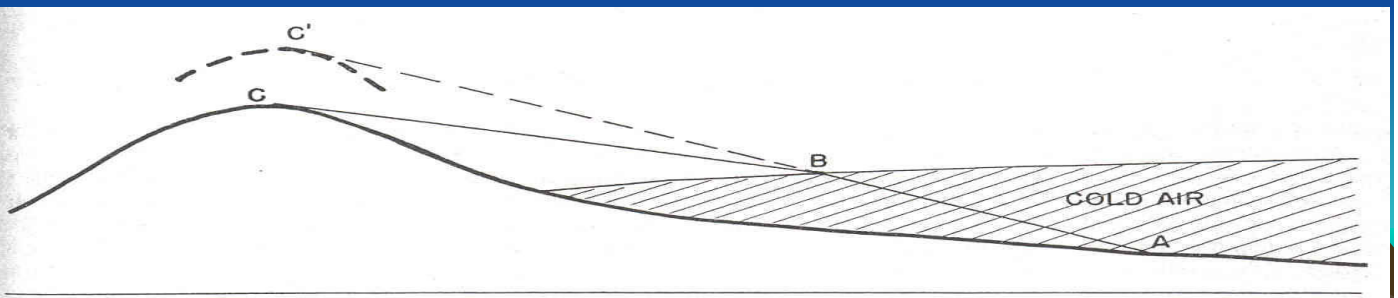

FIG. 7. Diagram showing distortion involving bending of light rays on passing from warm into cold air.

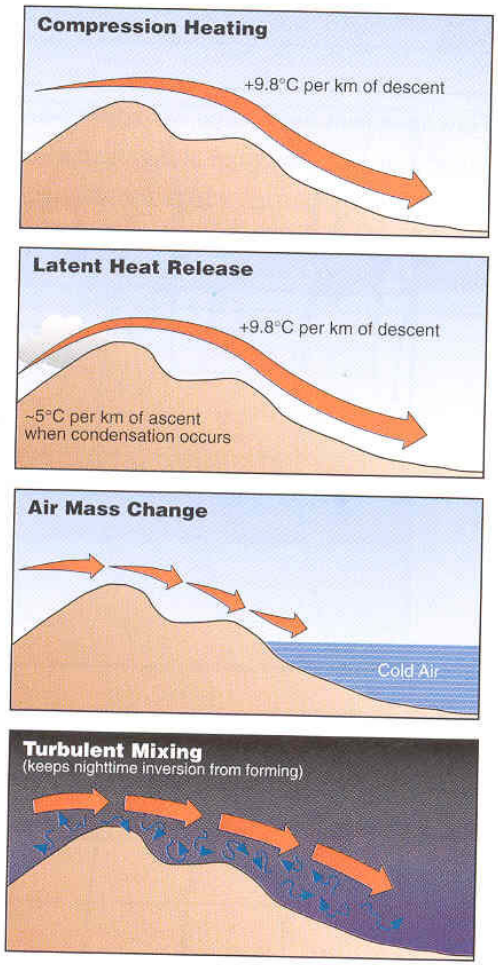

Figure 10.14 Four factors cause the warming and drying associated with chinooks. (Adapted from Beran, 1967)

Notable Boulder Windstorms

7-8 January 1969
- 130 mph at NCAR, 96 mph downtown
- 1 death

23 January 1971
- 147 mph at NCAR

11 January 1972
- wind gusts to 97 mph
- 40 trailers damaged
- $3 million damage

4 December 1978
- 148 mph at ?
- 1 death

17 January 1982
- 137 mph at NCAR
- 20 gusts above 120 mph in 45 min!
- At least 15 injuries
- $20 million damage, 40% of Boulder buildings damaged!

24 January 1982
- 140 mph at Wondervu

24 September 1986
- 131 mph at ?
- $100,000 damage

24 January 1992
- 143 mph (kt?) north Boulder

2-3 February 1999
- 127 mph at Sugarloaf, 120 mp in Lafayette, 119 mph in Wondervu, 100 mph in Longmont, 98 mph in Boulder
- $3 million damage

8-10 April 1999
- 120 mph at Sugarloaf, near 100 mph in south Boulder, 90 mph in Longmont
- $20 million damage from Pueblo to Fort Collins

From 1967-1995, winds > 100 mph occurred 35 times

Photos courtesy of UCAR

Damage in South Boulder from the 8 January 1969 windstorm (Ed Zipser)

Source: http://www.co.boulder.co.us/sheriff/pdf/oem/highwind.pdf and http://www.cdc.noaa.gov/Boulder/wind.html

Windstorm Damage

- According to RMIIA, Colorado's top five most costly windstorms are:
  - $20 million in insured damage occurred along the Front Range on April 8-10, 1999.
  - $20 million in insured damage occurred in Boulder County on Jan. 17, 1982.
  - $10 million in insured damage occurred along the Front Range on Jan. 28-29, 1987.
  - $5.2 million in insured damage occurred along the Front Range on Oct. 29, 1996.
  - $3 million in insured damage occurred along the Front Range on Feb. 2-3, 1999.

Observations from 1968 Field Project

JOINT FLIGHT SUMMARY, FEBRUARY 1968

Date	Area & Track	A/C Used	Upstream Winds: 500 mb	Upstream Winds: Tropopause	Wave Activity: Wavelength	Wave Activity: Peak-to-Peak Streamline Amplitude	Turbulence
13	Denver W	QA, T-33	240° 27kts	250, 55	Uncertain	Very weak	None
14	Pueblo WSW	T-33, B-57, U-2	220° 10kts	235, 40	15 km	400 m	Light
15	Denver W	QA, T-33, B-57, U-2	275° 48kts	260, 60	16 km (low levels)	2000 m (low)	Mdt. to severe in stratosphere.
16	Denver WNW	QA, T-33, B-57, U-2, Sailplane	280° 38kts	280, 75	15 km & longer	1600 m (low) 600 m (trop)	Mdt. low levels & stratosphere.
18	Denver WNW	QA, T-33, B-57, Sailplane	310° 39kts	320, 45	Irregular & 3-dimensional	300 m	Mdt. all levels
19	Denver W	QA, T-33, U-2	290° 55kts	310, 000	Irregular & 3-dimensional	2000 m (low)	Mdt. to severe low levels & stratosphe
20	Denver WNW	QA, T-33, B-57, Sailplane	285° 70kts	290, 90	11 km (low levels 45 km (tropopause)	2000 m (low) 1000 m (trop)	Light, Mdt. in rotors.
25	Denver WNW	QA, B-57, Comanche Sailplane	310° 50kts	290, 60	Single wave	800 m (low) 400 m (trop)	Light

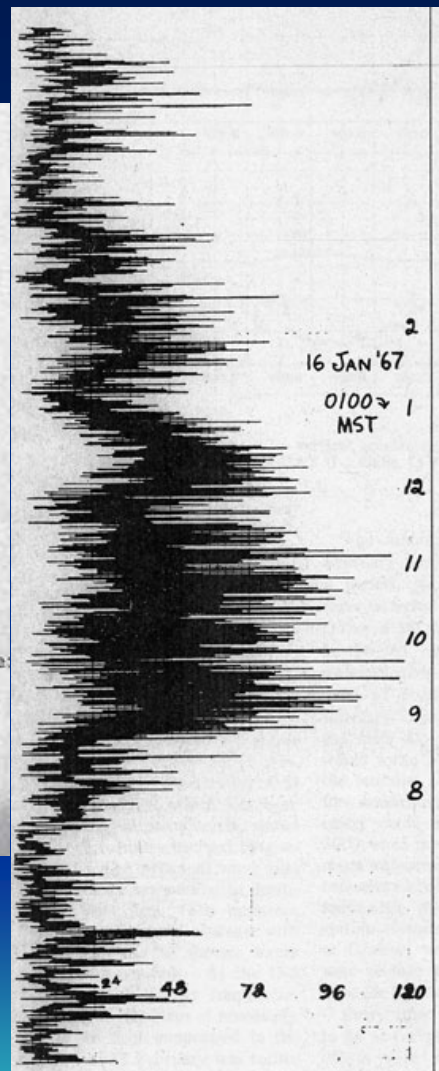

1967 Storm

Fig. 2. Recorded wind data from NCAR building in Boulder during a severe downdraft storm. Wind speed in mph, time in hours.

Figure from Kuettner and Lilly (1968)

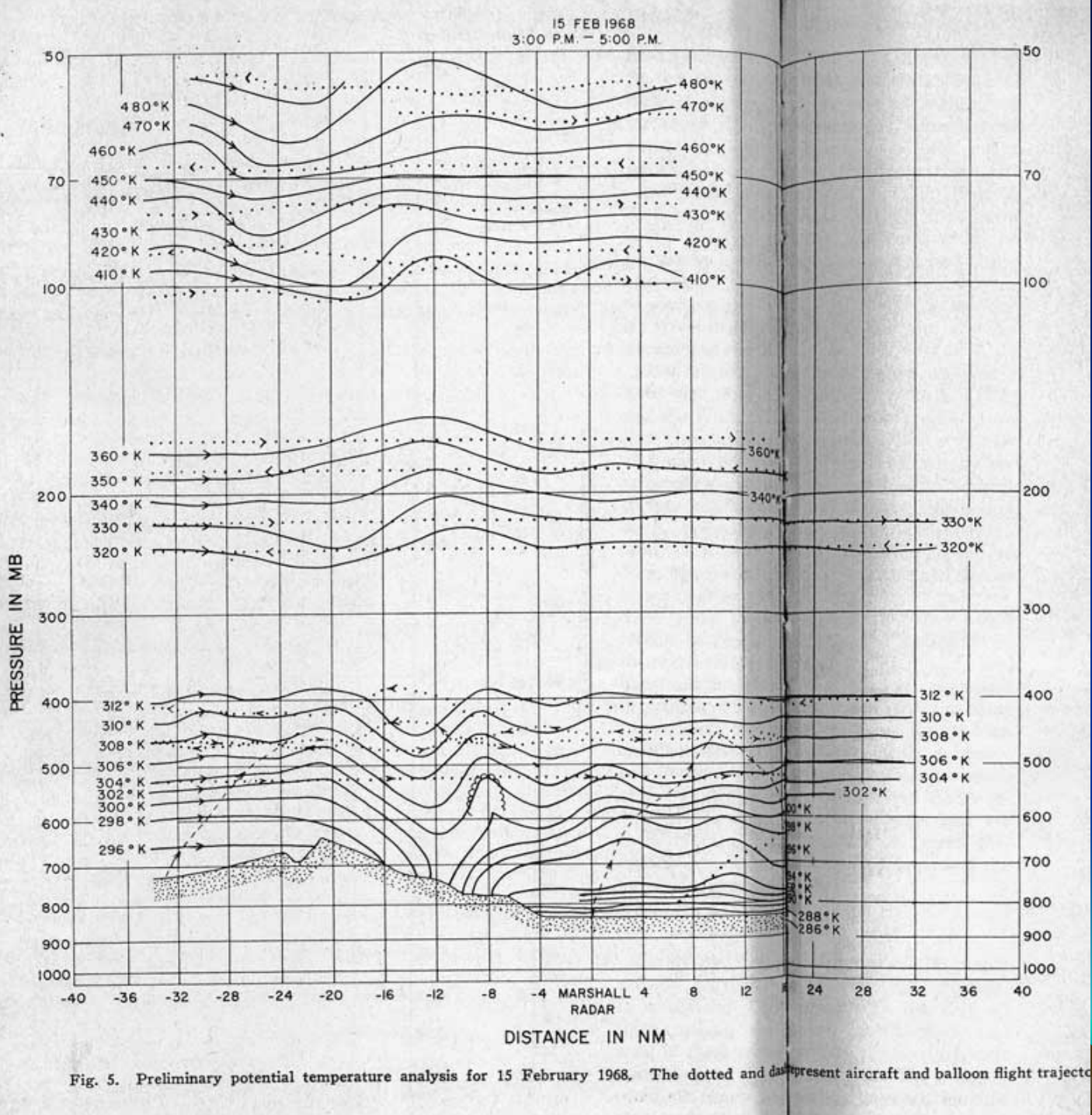

Fig. 5. Preliminary potential temperature analysis for 15 February 1968. The dotted and das present aircraft and balloon flight trajecto

Figure from Kuettner and Lilly (1968)

Data from a composite study

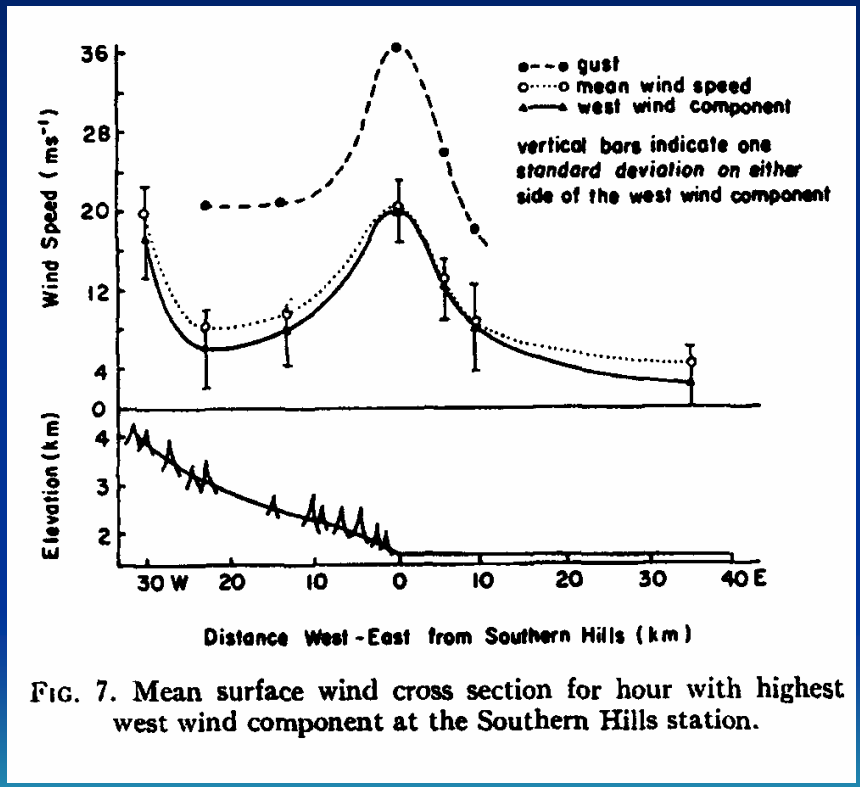

FIG. 7. Mean surface wind cross section for hour with highest west wind component at the Southern Hills station.

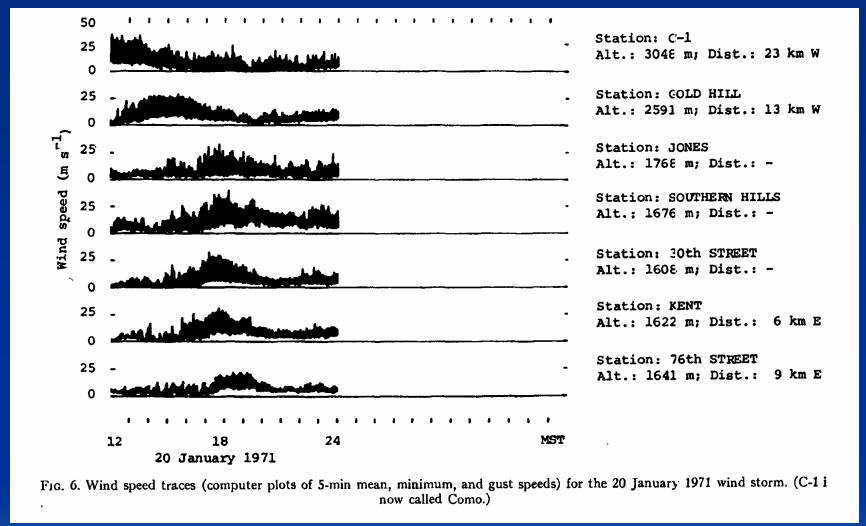

FIG. 6. Wind speed traces (computer plots of 5-min mean, minimum, and gust speeds) for the 20 January 1971 wind storm. (C-1 i now called Como.)

Figures from Brinkmann (1974)

Composite soundings at onset of Boulder windstorms

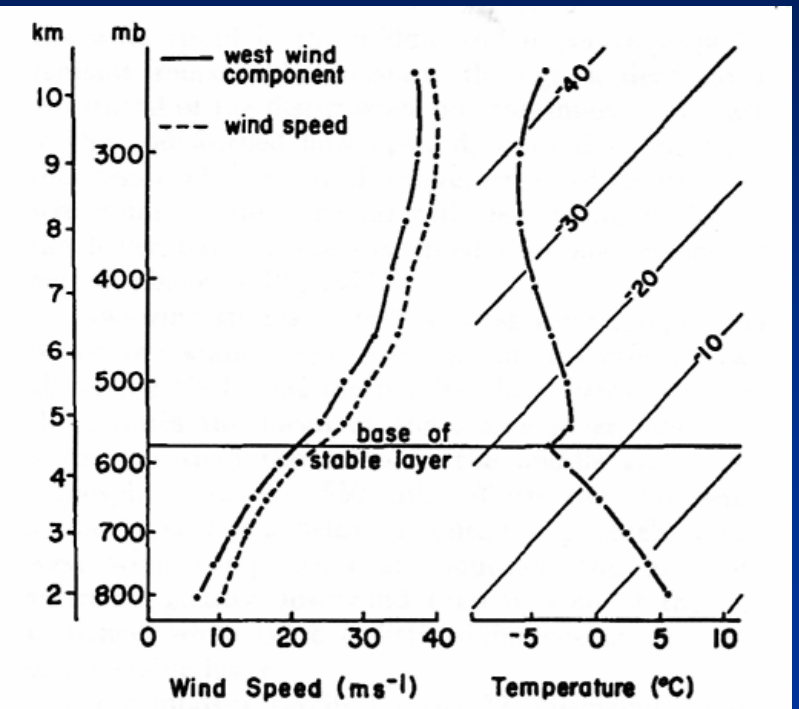

FIG. 14. Composite upwind sounding for time close to the beginning of wind storms in Boulder.

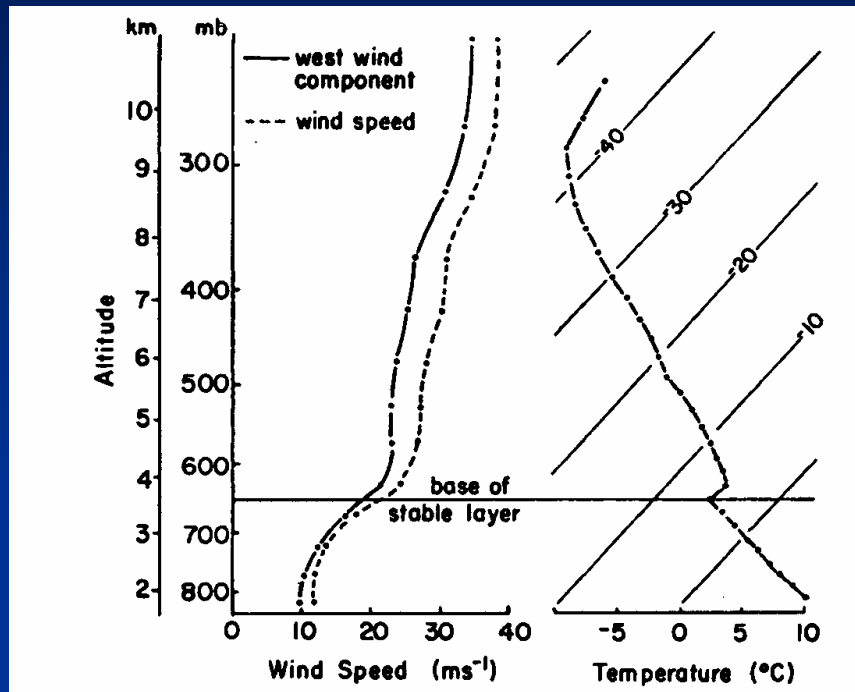

FIG. 15. Composite Denver sounding for time close to or during wind storms in Boulder.

Note that base of isothermal level is 575 in the upstream sounding, but is lower (650 mb) in the downstream sounding.
Also, downstream sounding has steeper lapse rate, higher θ at lower levels

Figures from Brinkmann (1974)

Composite Denver soundings for different types of windstorms

- Downstream sounding composites
  - Inversion level averages ~675 mb for Boulder wind cases
  - ~625 mb for slope wind cases

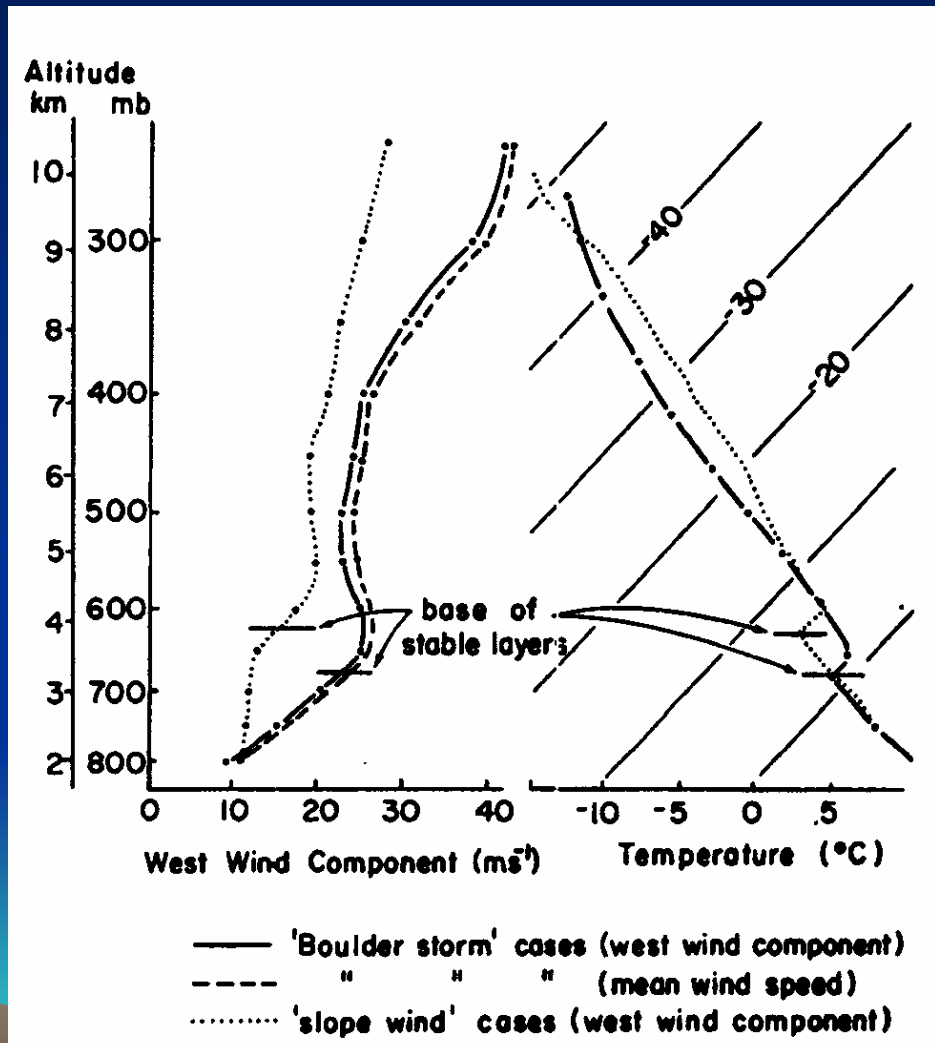

FIG. 16. Composite Denver sounding for time of storms in Boulder and winds on the slopes.

Figures from Brinkmann (1974)

Observations from the 11 January 1972 Windstorm

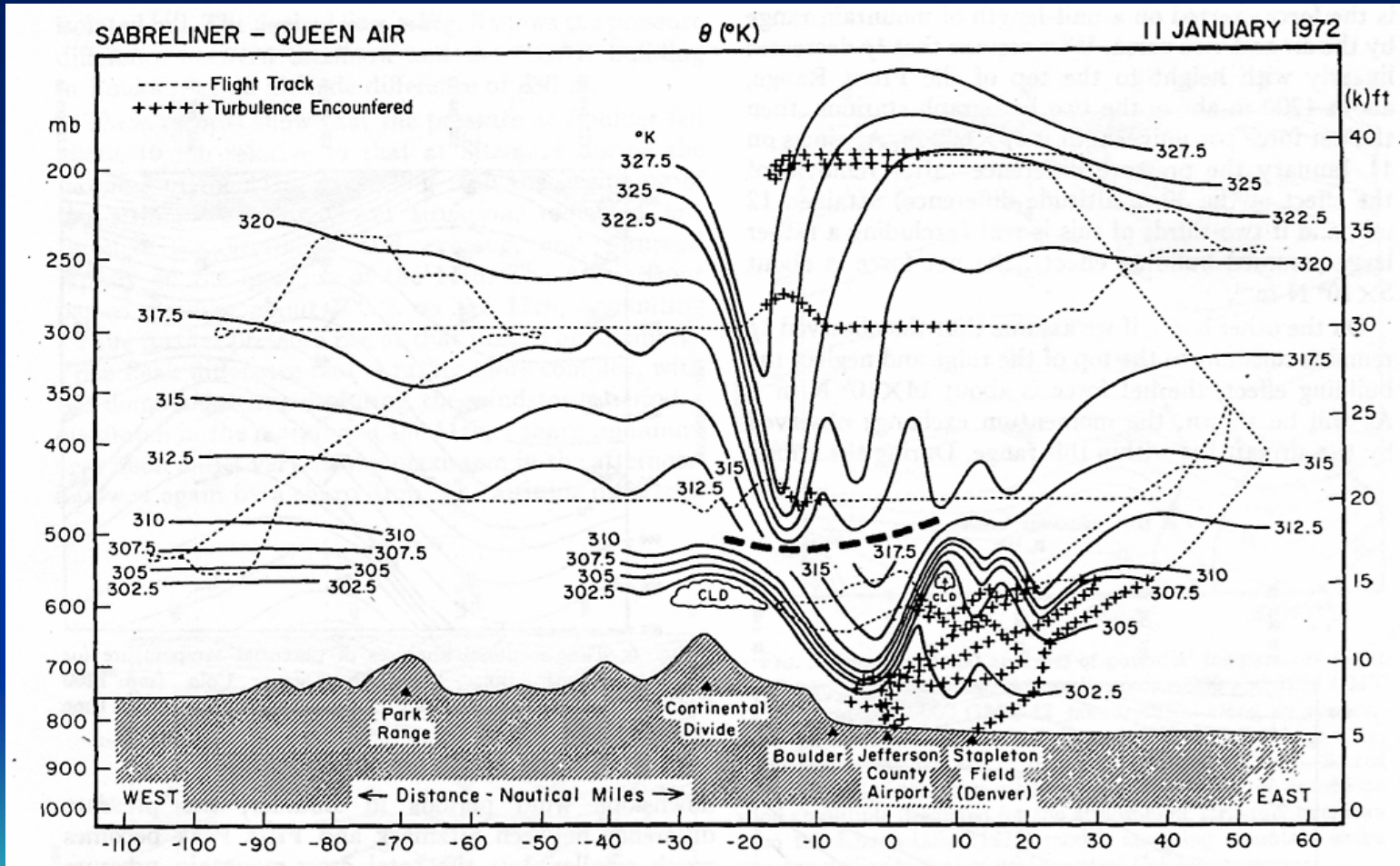

FIG. 7. Analysis of the potential temperature field (solid lines) from aircraft flight data and sondes taken on 11 January 1972. The dashed lines show aircraft track, with periods of significant turbulence shown by pluses. The heavy dashed line separates data taken by the Queen Air at lower levels before 2200 GMT from that taken by the Sabreliner in the middle and upper troposphere after 0000 GMT (12 January). The aircraft flight tracks were made along an approximate 130°–310° azimuth, but the distances shown are along the east-west projection of those tracks.

Figure from Lilly (1978)

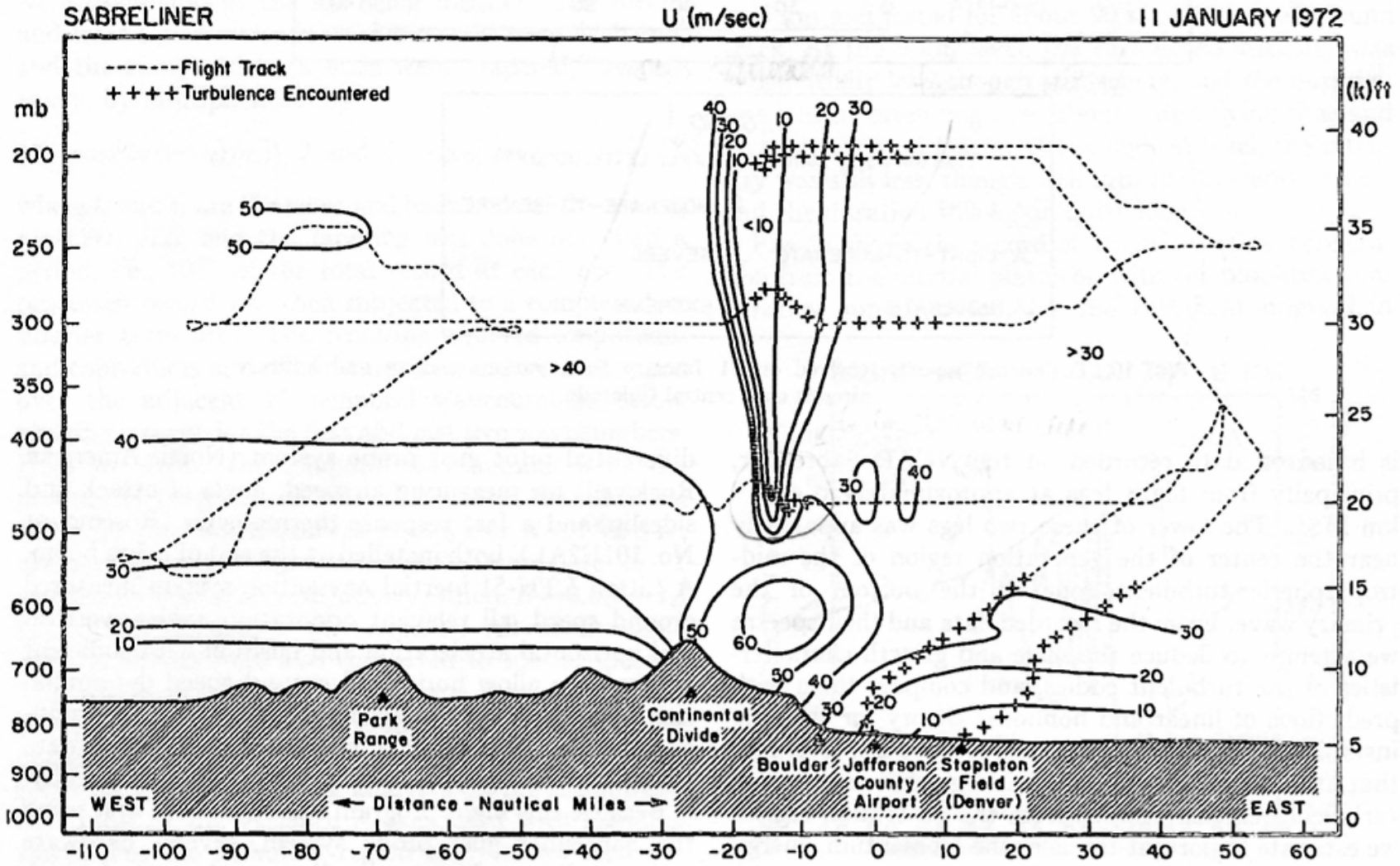

FIG. 9. Analysis of westerly wind component (m s^{-1}) on 11 January 1972, made from Sabreliner and sonde data only. The analysis below 470 mb over the eastern slope was deduced from assumptions indicated in the text.

Figure from Lilly (1978)

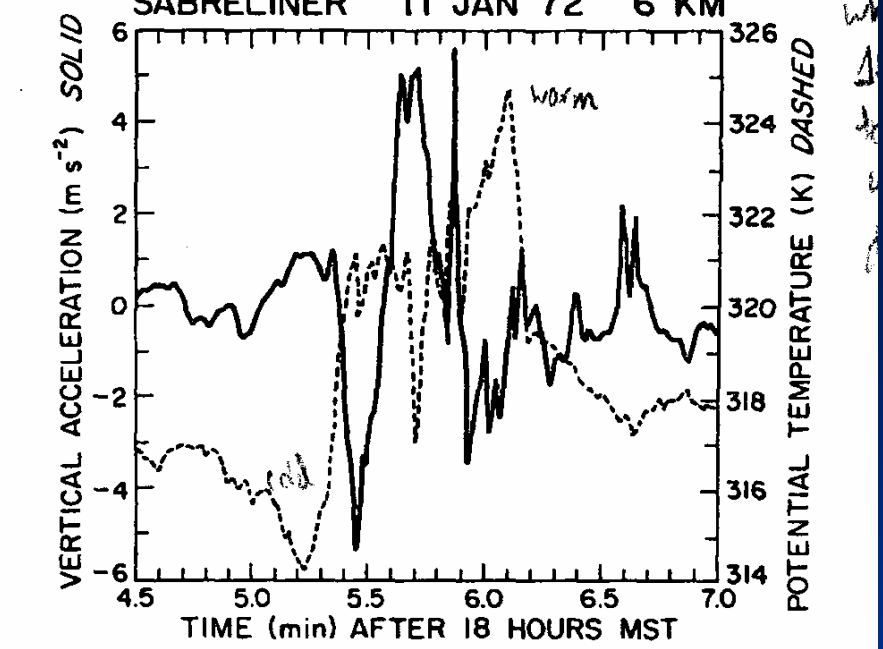

FIG. 11. Vertical acceleration (solid) and potential temperature (dashed) from the Sabreliner flight record at the 6 km level in the strong turbulence zone just east of the mountain crest. All data are averaged over 1 s intervals.

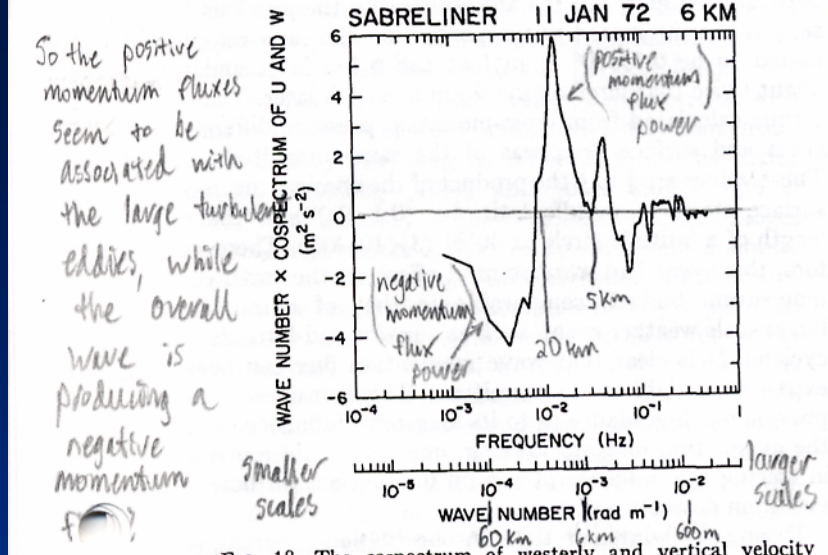

FIG. 18. The cospectrum of westerly and vertical velocity components, multiplied by wavenumber, for the entire 6 km flight leg.

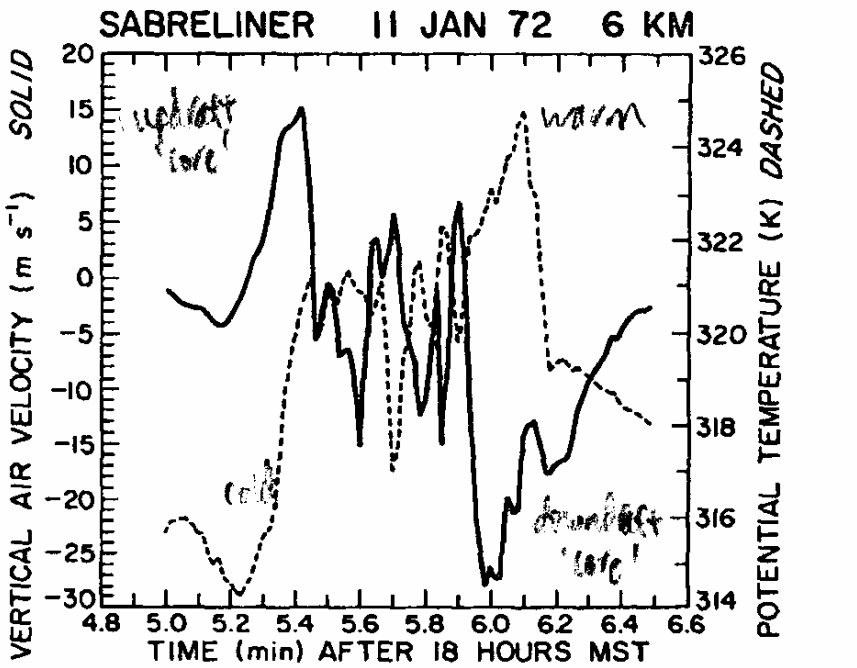

FIG. 12. Vertical velocity (solid) and potential temperature (dashed) in the turbulent zone at 6 km.

Figures from Lilly (1978)

- Pressure traces during a windstorm
- Note in particular the sudden pressure drop at Boulder during the storm
- Is this causing the high winds?

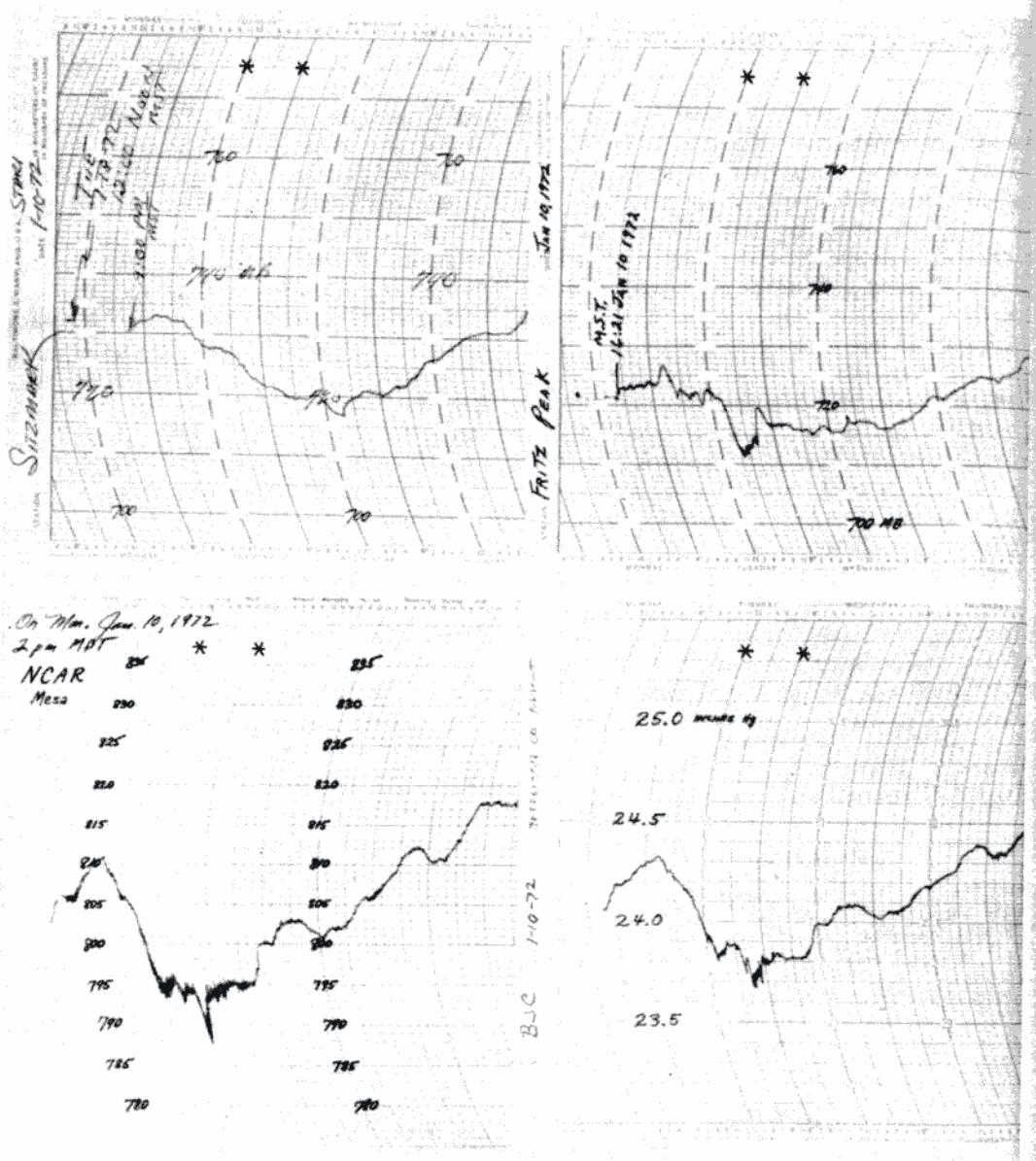

Fig. 7. Four microbarograph traces from the Front Range area on 11 January 1972. Upper left: western side of Continental Divide at about 9000 ft. Upper right: eastern side of Divide at about 9000 ft. Lower left: NCAR site at 6100 feet. Lower right: Jefferson County Airport at 5500 ft. See Fig. 2 for exact locations. All records are in millibars except for the last, which is in inches of Hg. Note asterisks placed on chart to indicate noon and midnight on the 11th.

Figure from Lilly and Zipser (1972)

Downslope Windstorm Mechanisms

There are 3 proposed mechanisms for downslope windstorms:

1. Develop when the flow over a mountain transitions from subcritical -> supercritical over the mountain, analogous to a hydraulic jump
2. Large-amplitude vertically-propagating mountain waves that undergo partial reflection at interfaces – properly 'tuned' waves resonate with increasing amplitude
3. Wave breaking and wave-induced critical layers

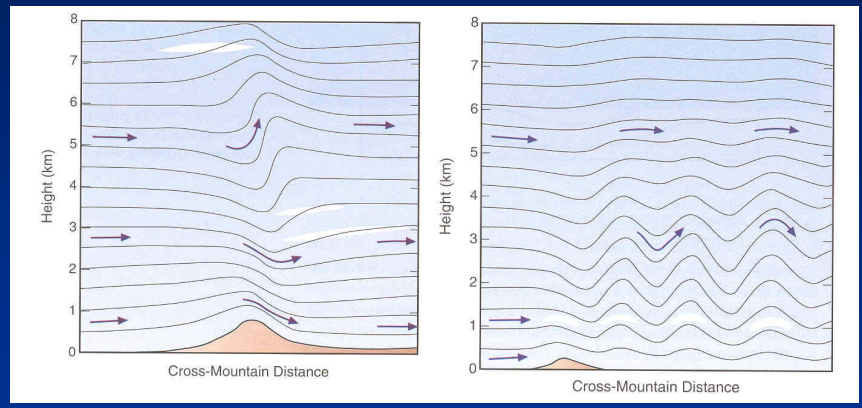

Vertically propagating waves with large amplitude

Trapped lee waves undergoing reflection

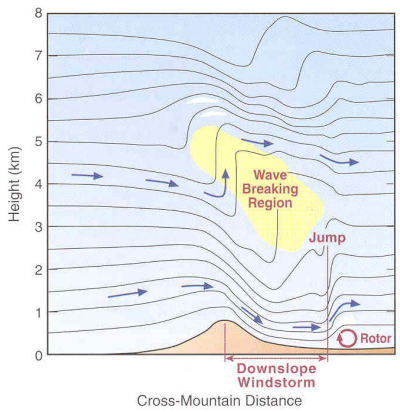

Figure 10.11 Hydraulic flow produces a distinctive flow pattern in the lee of a mountain barrier that is characterized by a region of wave-breaking aloft and a sudden jump in the streamline pattern (*hydraulic jump*) downwind of the barrier. A turbulent rotor cloud may form behind the hydraulic jump. Downslope windstorms may occur during hydraulic flow. (Adapted from Carney et al., 1996)

Figures from Whitefield (2000)

Long's Hydraulic Jump (1953a)

- Homogeneous fluid flowing over ridge-like obstacle. Assume flow is in hydrostatic balance and bounded by free surface.
- Consider y-independent motions
- Assume steady-state flow.

$$u\frac{\partial u}{\partial x}+g\frac{\partial D}{\partial x}+g\frac{\partial h}{\partial x}=0$$

Where D is the thickness of the fluid and *h* is the obstacle height.

Using the continuity equation

$$\frac{\partial (uD)}{\partial x}=0$$

we get:

$$(1-\frac{1}{Fr^2})\frac{\partial (D+h)}{\partial x}=\frac{\partial h}{\partial x}$$

where

$$Fr^2=\frac{u^2}{gD}$$

Most people Interpret Fr^2 as the Froude #. Here it is a ratio of the fluid speed to the propagation speed of shallow linear gravity waves

So the free surface can either rise or fall depending on the magnitude of Fr^2

Supercritical case

Fluid thickens and slows as it crosses top of obstacle, minimum speed at crest

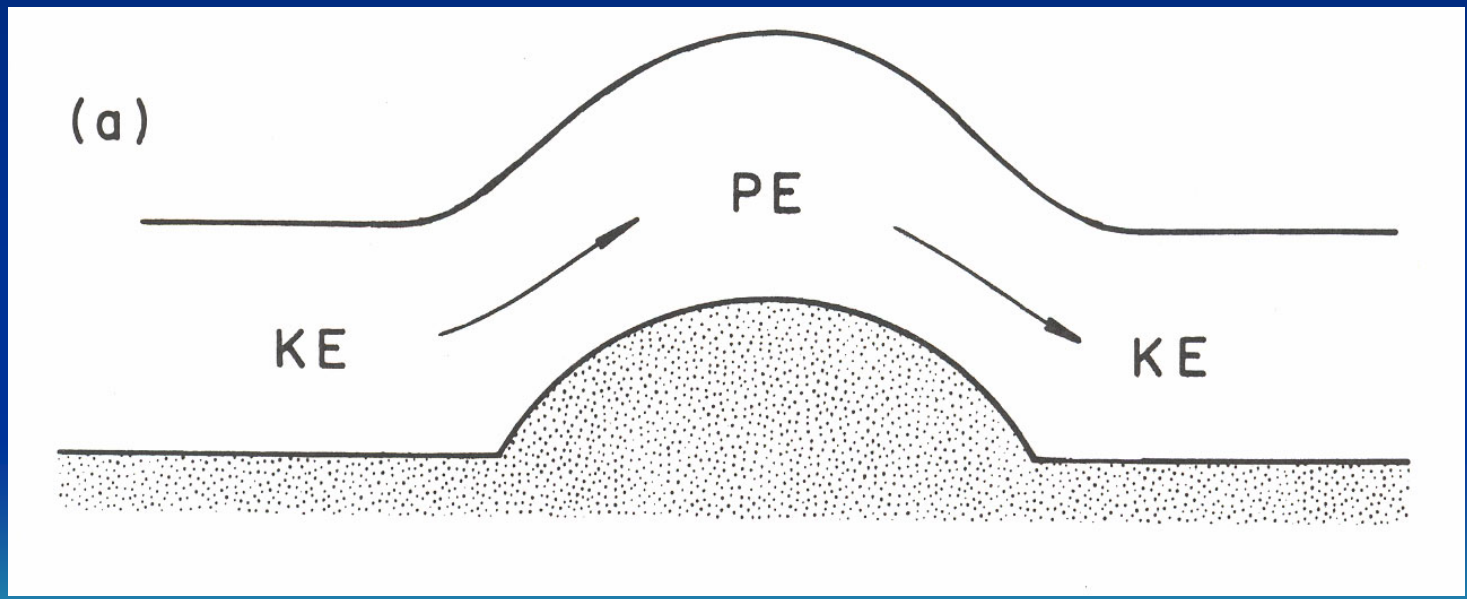

Schematic from Durran (1990)

Subcritical case

Fluid thins and accelerates as it crosses top of obstacle, reaches maximum speed at crest

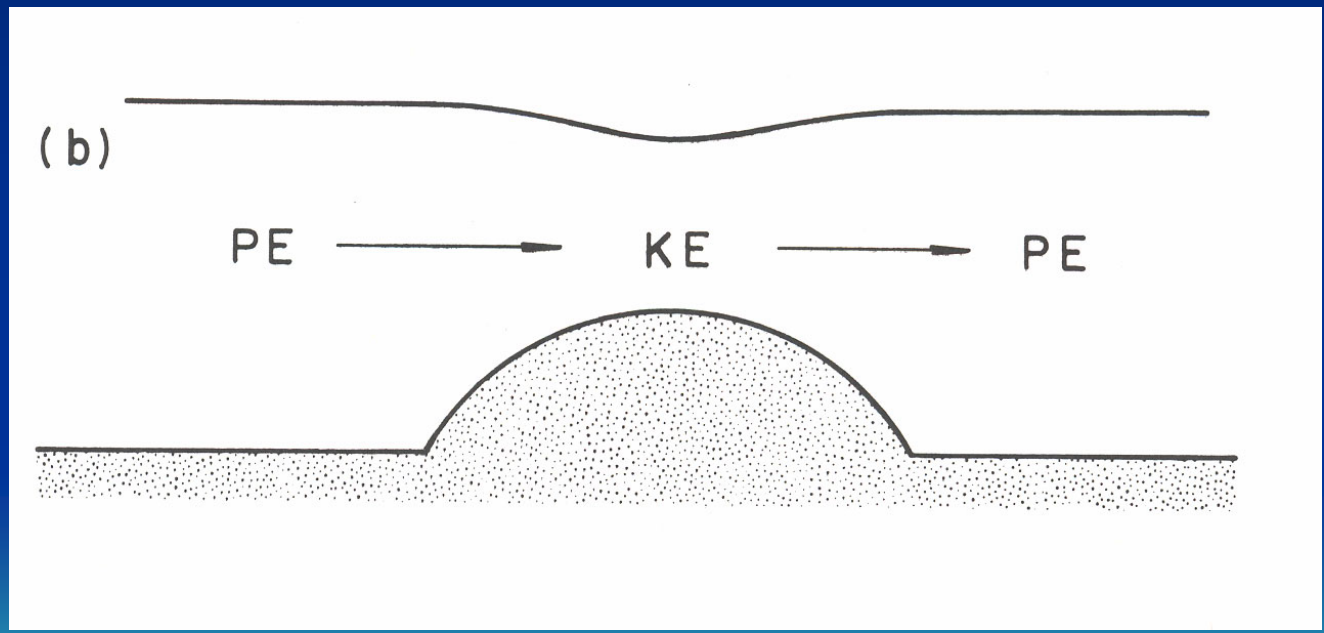

Schematic from Durran (1990)

Hydraulic jump case

Flow transitions from subcritical to supercritical at top of obstacle, potential energy is converted to kinetic energy over the entire barrier

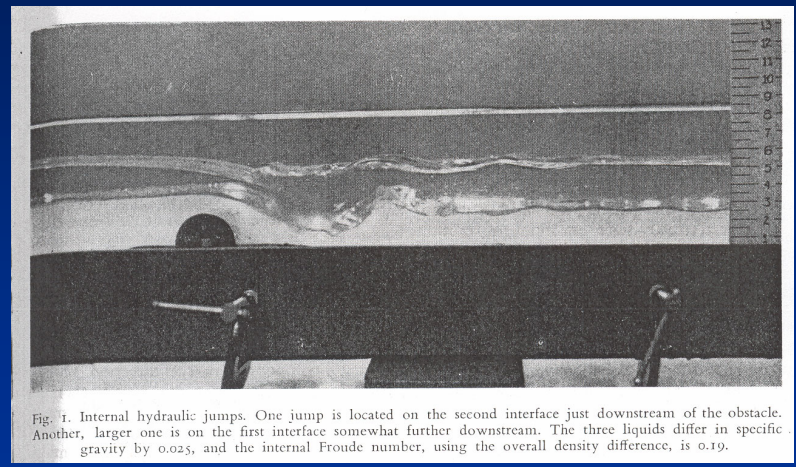

Fig. 1. Internal hydraulic jumps. One jump is located on the second interface just downstream of the obstacle. Another, larger one is on the first interface somewhat further downstream. The three liquids differ in specific gravity by 0.025, and the internal Froude number, using the overall density difference, is 0.19.

Figure from Long (1953a)

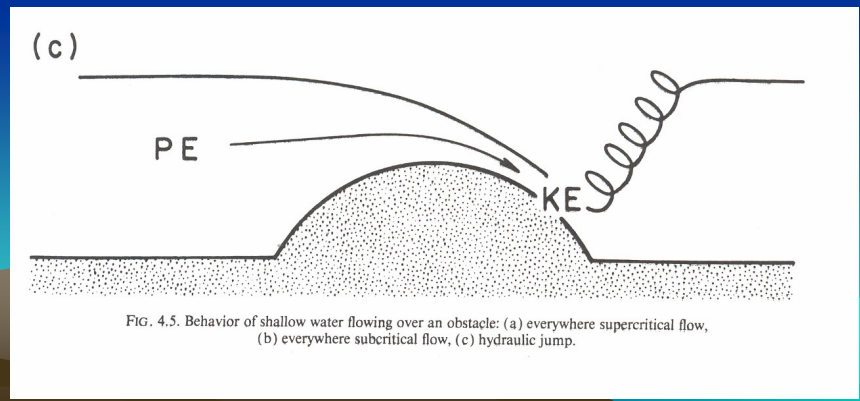

FIG. 4.5. Behavior of shallow water flowing over an obstacle: (a) everywhere supercritical flow, (b) everywhere subcritical flow, (c) hydraulic jump.

Schematic from Durran (1990)

Forecasting

There appear to be at least three mechanisms which can cause the flow to undergo transition from subcritical to supercritical:

1. Wave breaking - in an atmosphere with constant N and u_0; mountain large enough to cause breaking waves (Clark and Peltier 1977)
2. Scorer-parameter layering – in an atmosphere with constant u_0 and two layers of N: mountain too small to cause breaking waves (Durran 1986a)
3. Capping by a mean-state critical layer: in an atmosphere with constant N and u_0 below a critical layer, where in the absence of the critical layer, the mountain is too small to cause breaking waves

Other mechanisms: wave-induced critical layers?

General development characteristics

- For the case of deep cross-mountain flow and no mean-state critical layer, observations suggest a windstorm will occur when:
  - Wind is directed across mountain (within 30° of perpendicular to ridgeline) and wind at mountaintop level exceeds a terrain dependent value of 7 to 15 m s^{-1}
  - Upstream temperature profile exhibits an inversion or a layer of strong stability near mountaintop level (Colson 1954; Brinkmann 1974)

These conditions favor development of a downslope storm by creating conditions similar to Scorer parameter layering. They also promote the development of larger amplitude mountain waves, increasing the chances for breaking waves. Breaking waves are favored when the upper tropospheric winds are not too strong.

The effect of a mountaintop inversion

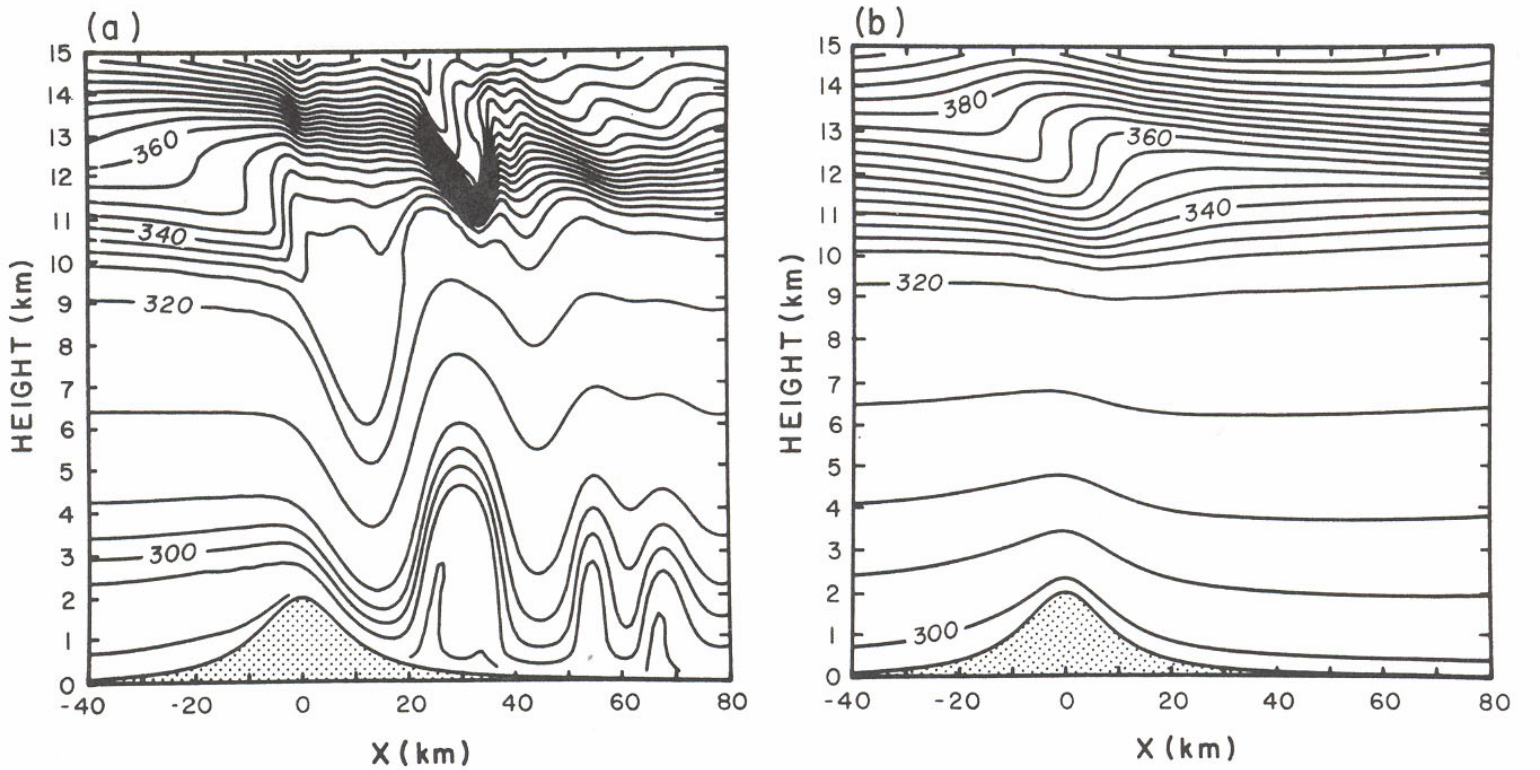

FIG. 4.10. (a) Isentropes form a simulation of the 11 January 1972 Boulder windstorm using the upstream conditions observed at Grand Junction, at a model time of 12 000 s. (b) As in (a), except that the upstream sounding has been modified to remove the elevated inversion. (From Durran 1986a.)

Figure from Durran (1990)

Other forecast factors

- Ideal terrain for windstorms are long ridges with gentle windward slopes and steep lee slopes (effective terrain shape can be modified by upstream blocking)
- Low humidity is better (moisture seems to reduce amplitude)
- Nighttime or early morning more likely (stability changing during this time?)
- Klemp and Lilly (1975) found that the strongest downslope events occur in Boulder when a one-half wavelength phase shift was present between ground and tropopause (partial reflection mechanism of linear theory)
- Durran (1986a) ran simulations of the 11 January 1972 event – this condition appears necessary, but not sufficient for strongest windstorms
- Elevated inversions might be required for breaking waves to form
- Lee et al (1989) found that the presence of cold pools in the lee of the mountain could have a strong determinant in whether downslope winds would make it to the mountain base – it also altered the overall structure of the mountain wave in simulations (different lower boundary, change in scale?)
- In some cases, precipitation effects could play a role? (e.g. the 3 July 1993 Fort Collins windstorm case)

25 October 1997 Blowdown Event West of the Park Range

- 13,000 acres of old growth trees blown down in Mount Zirkel Wilderness Area/Routt National Forest, trees stacked 30 feet high, hunters trapped for 2 days; strongest winds lasted ~30 min
- Wind gusts exceeded 100 mph for 7 hrs at Arapahoe Basin Ski Area (el. 12,500 ft; peak gust 114 mph out of the east, windchill to -60°F)
- Factors: strong synoptically-driven flow from east to west (blizzard of ’97), an unusually cold and stable layer on the windward side of the mountains

Picture courtesy U.S. Forest Service

For more, see Meyers et al (2003)

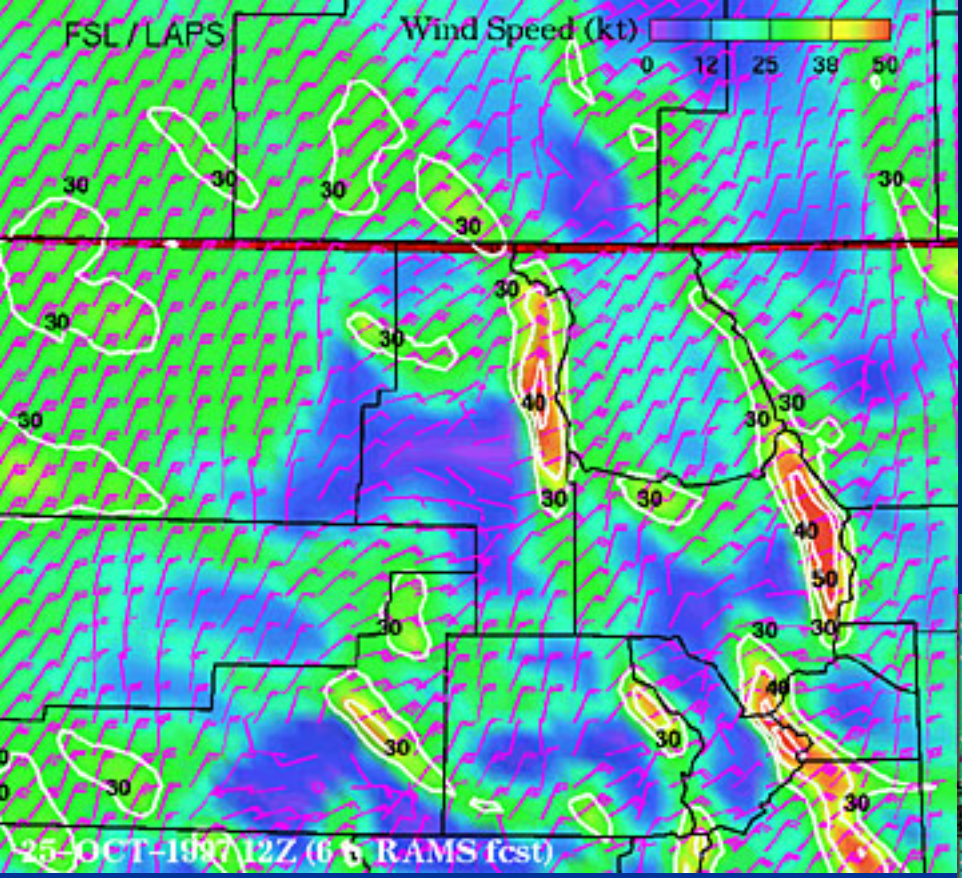

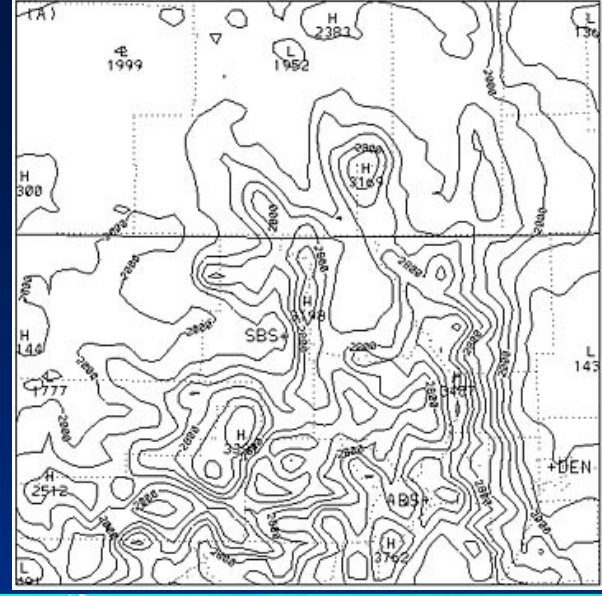

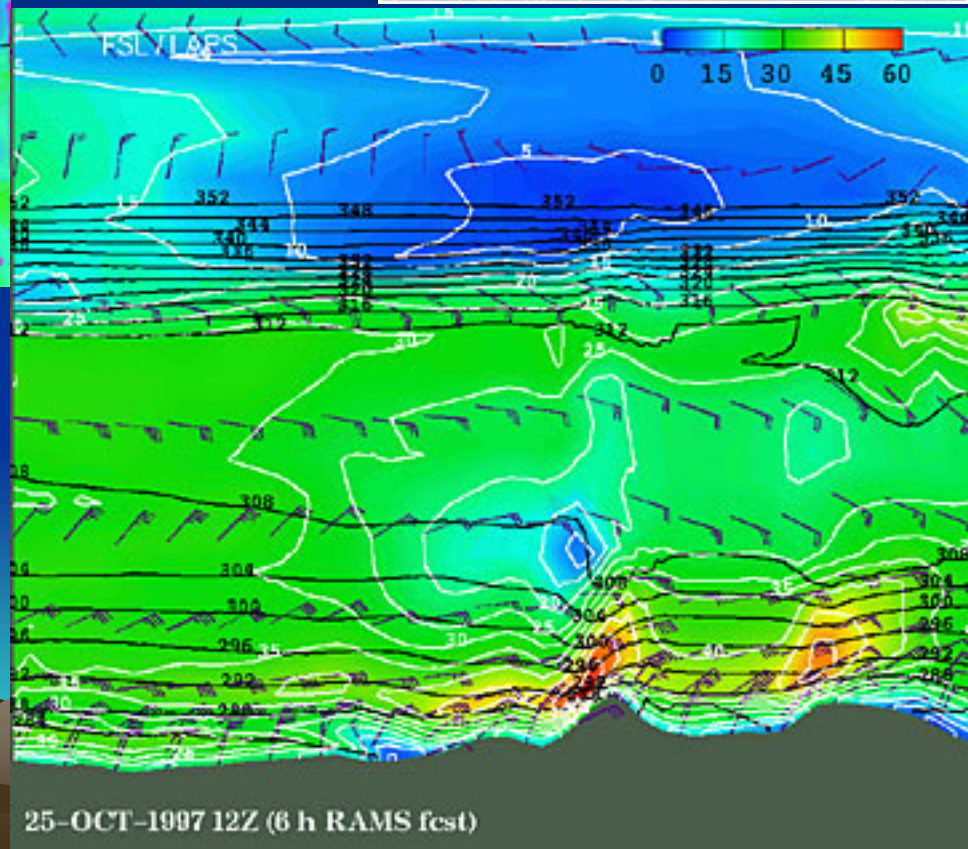

RAMS Model Simulation
Figures from FSL Forum, Feb. 1999

(Wind speed in knots, height in meters)

Historical Fort Collins Windstorms

Fort Collins Windstorms noted in conjunction with Boulder Windstorms
(as reported in the Boulder Daily Camera)

- Dec. 4-5, 1880
- Mar. 18, 1920
- May 21, 1925 also including Eaton, Greeley, Windsor, and Platteville
- Jan. 15, 1943 including Loveland, Ft. Morgan
- Dec. 20, 1948 average wind of 41 mph, gust to 96 mph
- Dec. 6, 1963 Fort Collins, Greeley, Sterling
- Jan 27-28, 1965 gust to 73 mph
- Feb. 13-14, 1967
- Dec. 6, 1967 gust to 66 mph
- Dec. 21-22, 1969 Larimer County
- Nov 30-Dec 1, 1970
- Mar 31, 1971 Ft Collins and Laporte, 40-50 mph, gusts to 72 mph, one fatality and several injuries in Fort Collins
- Jan 11-12, 1972 Fort Collins Loveland and just about everywhere
- Nov 25-26, 1972 Fort Collins

Data from Whiteman and Whiteman (1973)

Fort Collins Windstorm Climatology

- Peak windstorm season is during the winter months
- Windstorms often occur in ‘streaks’; Jan. 1977 had 7 separate events!
- Summer events are rare, but not unprecedented (June 1973, July 1993)

Most or all of the data is from old Foothills campus station

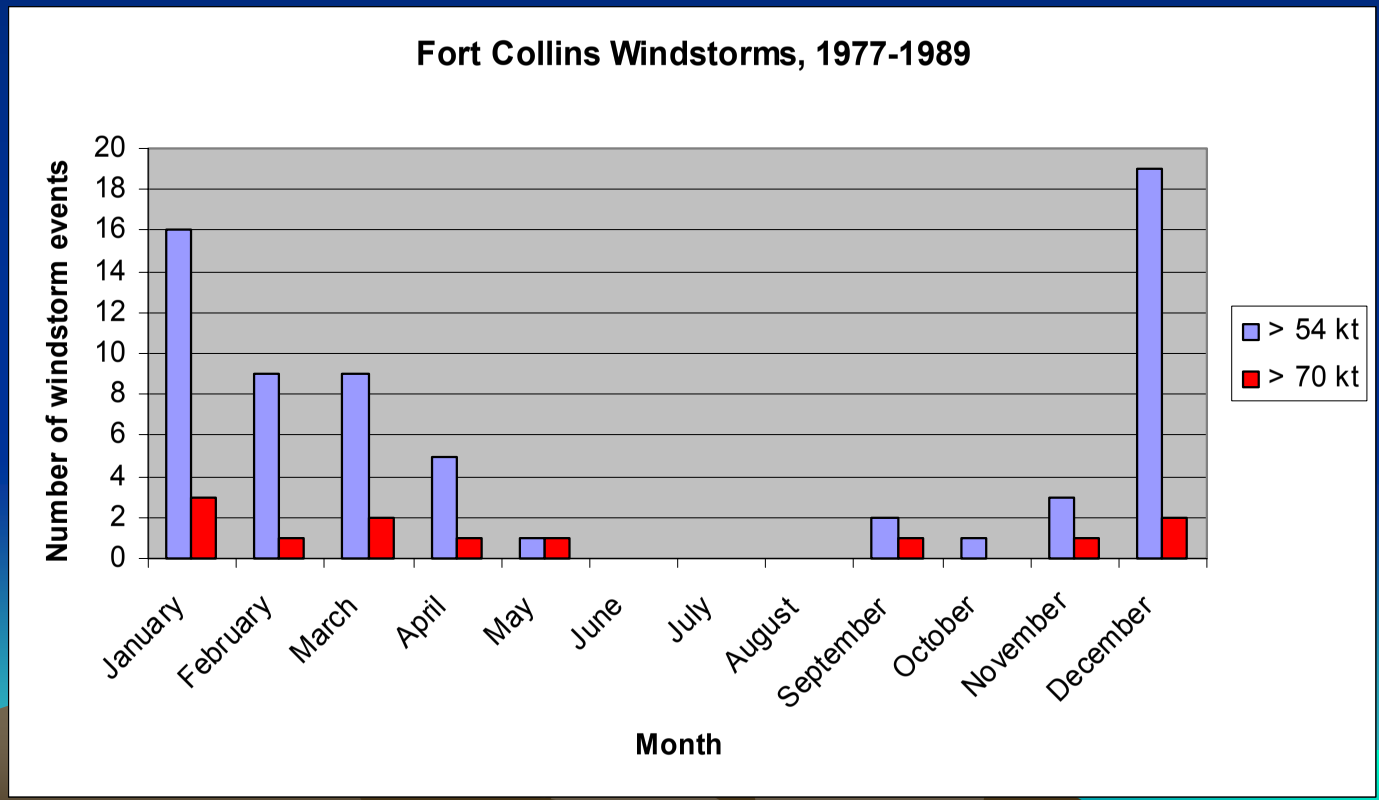

Data courtesy of John Weaver (see Lee et al 1989; Weaver and Phillips 1990)

- For comparison, the seasonal cycle of Boulder winds

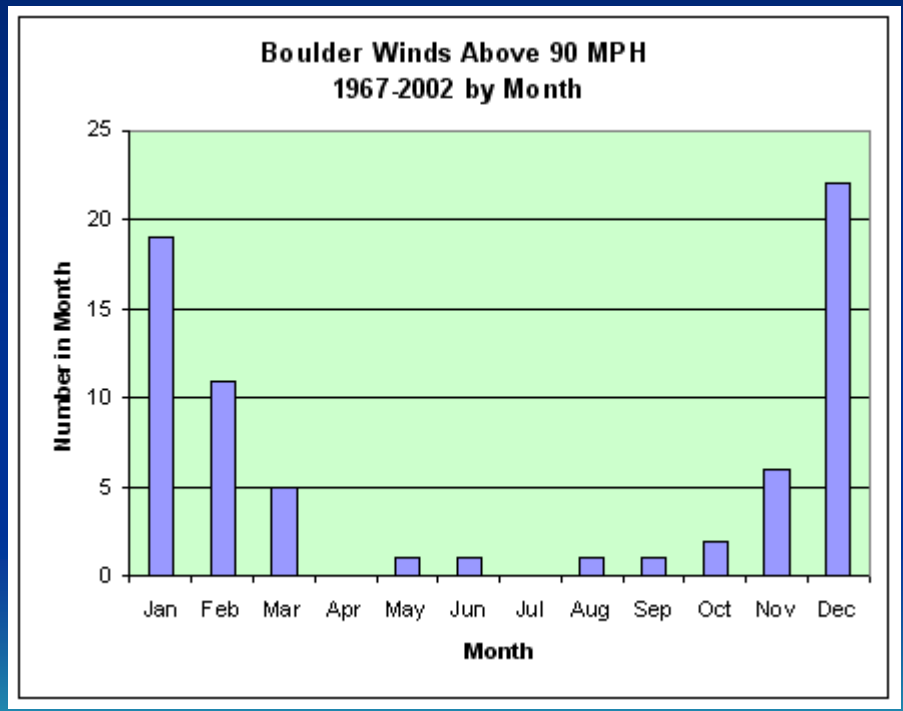

Source: http://www.bcna.org/winds.html

FC Windstorm Climatology, cont'd

- 65 windstorms with max gusts >54 kt (~5 per year)
- 12 windstorms with max gusts >70 kt (~1 per year)

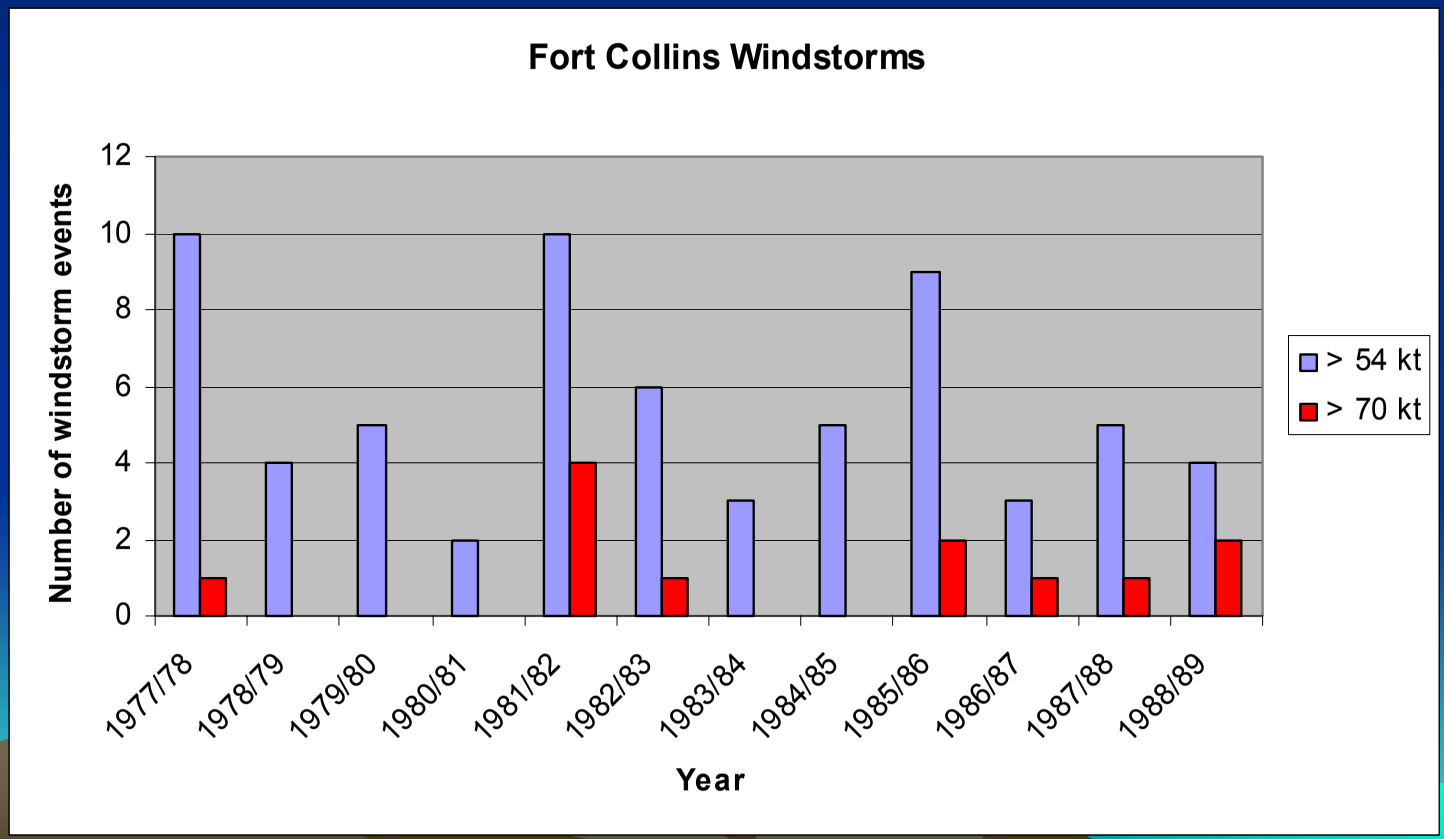

Data courtesy of John Weaver (see Lee et al 1989; Weaver and Phillips 1990)

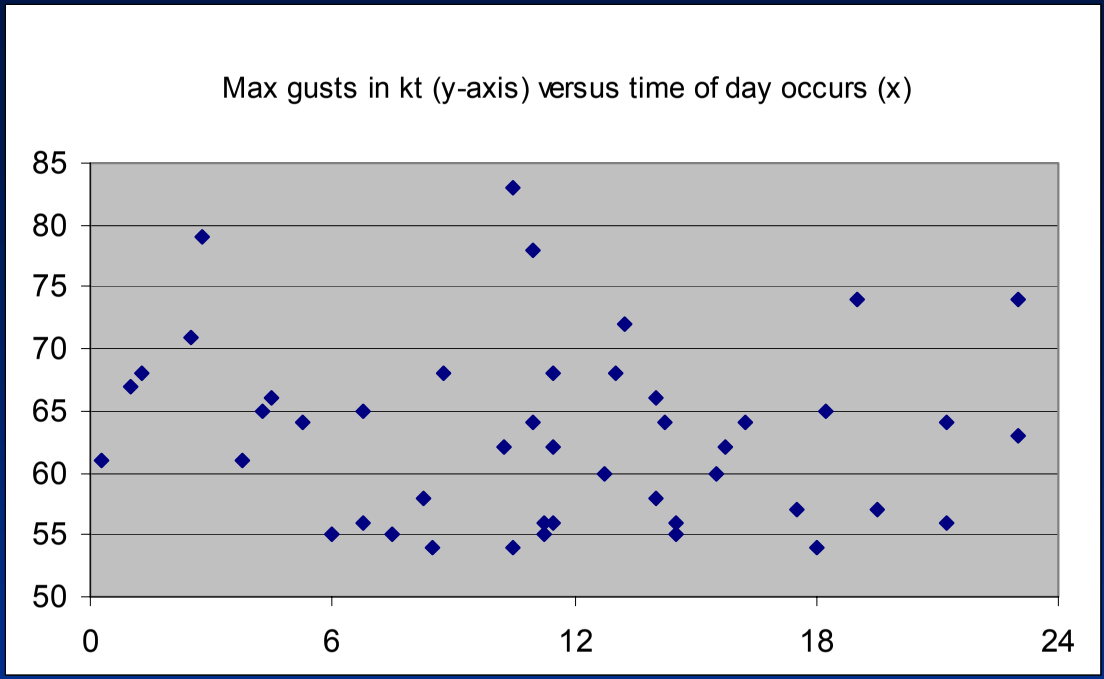

Note that there is no preferential time of year for maximum gusts

Max gusts occur during all parts of the day, with a weak peak around midday

Average windstorm duration is 8 hrs (min of 1.25 h, max of 20 h)

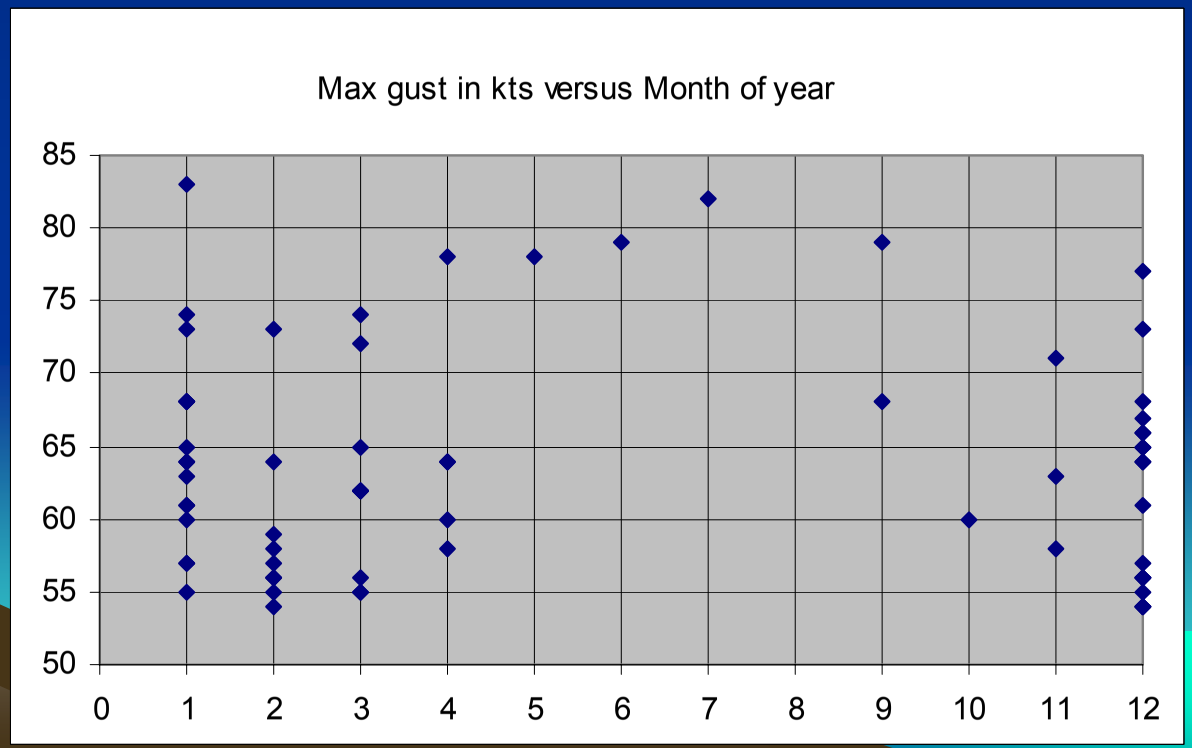

Data courtesy of John Weaver (see Lee et al 1989; Weaver and Phillips 1990)

Wind trace of windstorm at Fort Collins

Note that winds are much steadier than Boulder storms

Trace courtesy of Richard Johnson

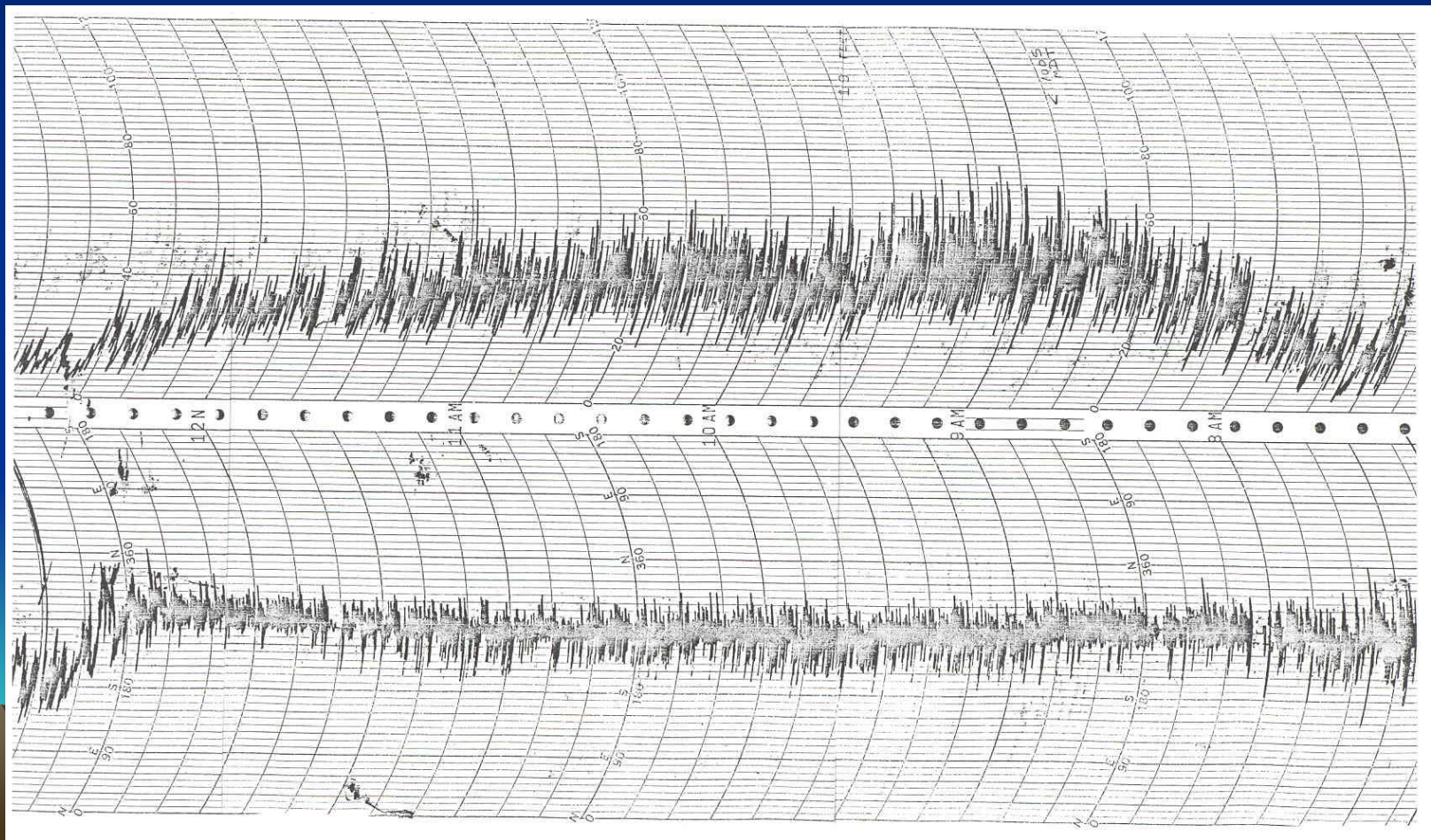

Notable Fort Collins Windstorms

Most or all of the data is from the old Foothills campus station, data after 1988 is from Christman Field station

Date	Strength of max gust (kt)
17/18 Jun 1973	79
26 Nov 1977	71
3 Jan 1982	74
24 Jan 1982	83
29/30 Mar 1982	74
2 Apr 1982	78
30 Mar 1983	72
15 Feb 1986	73
4/5 May 1986	78
28/29 Jan 1987	73
2 Dec 1987	73
18 Sep 1988	79
22 Dec 1988	77
3 Jul 1993	82

Data courtesy of
John Weaver
(see Lee et al 1989;
Weaver and Phillips 1990)

Rotors

Rotor: a region of reversed flow

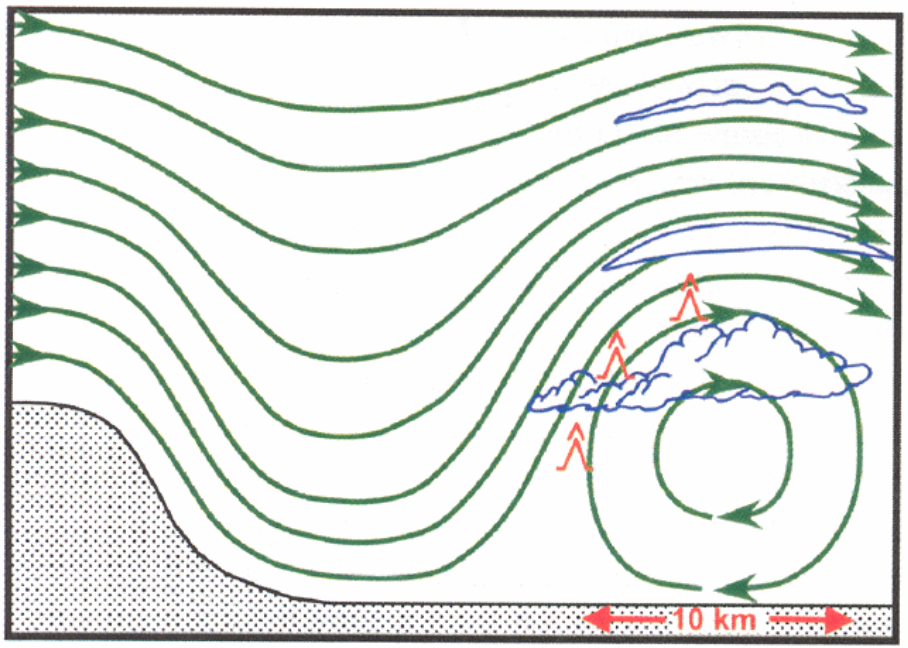

FIG. 2. Schematic streamlines illustrating a rotor circulation and attendant cloud features (adapted from Ludlam and Scorer 1957). Regions of clear-air turbulence associated with the rotor circulation are denoted by the red symbols.

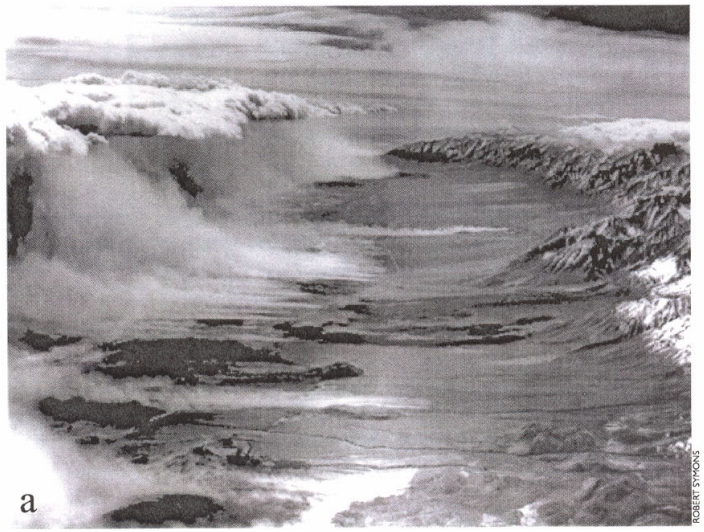

FIG. 1. Photographs over the Owens Valley in the lee of the Sierra Nevada Range, taken during the Sierra Wave Project, illustrating (a) and (b) common rotor characteristics such as rotor and lenticular clouds and (a) blowing dust. The flow in both photographs is from right to left as viewed from the north.

a, and particularly
y are notorious for
). Rotors have also

atory, Monterey,
Seattle, Washington
, Naval Research
ce Hopper Avenue,

Figures from Doyle and Durran (2004)

A Unique Observation

FIG. 4. One of two Pratt–Read sailplanes of the Sierra Wave Project at a runway in Bishop, CA. (From Harold Klieforth's private collection.)

Figure from Grubiši and Lewis (2004)

"On another occasion (25 April 1955) a unique observation of the rotor circulation was made when the Sierra Wave Project sailplane broke apart in severe turbulence near the upwind edge of the roll cloud and the pilot, Mr. Larry Edgar, descended through this region by parachute. After being carried rapidly down the direction of the main stream eastward across the Valley below the roll cloud, he encountered a layer of calm air at about 2,500 m (1,300 m above the ground) below which he drifted westward in a wind estimated at 25 knots. He finally landed on the *west* side of the Owens Valley below the leading edge of the roll cloud."

-- Quote from Scorer and Klieforth (1958)

Rotor observations from Sierra Wave Project

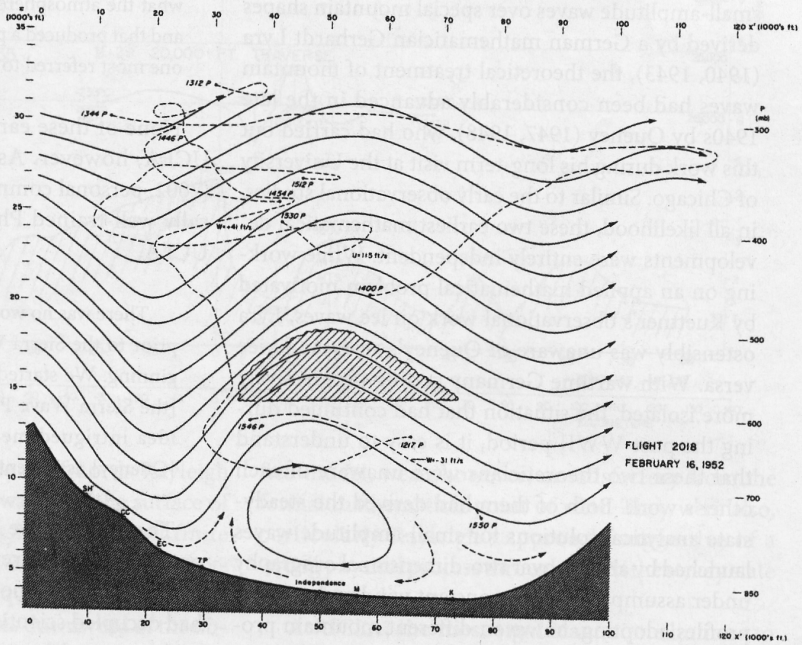

Fig. 3.28

FIG. 5. Streamlines in a strong mountain wave and "normal" rotor on 16 Feb 1952. Dashed lines (without arrows) show the sailplane trajectory projected onto a west-to-east vertical cross section perpendicular to the axis of the Owens Valley near Independence. (From Holmboe and Klieforth 1957.)

Figure from Grubiši and Lewis (2004)

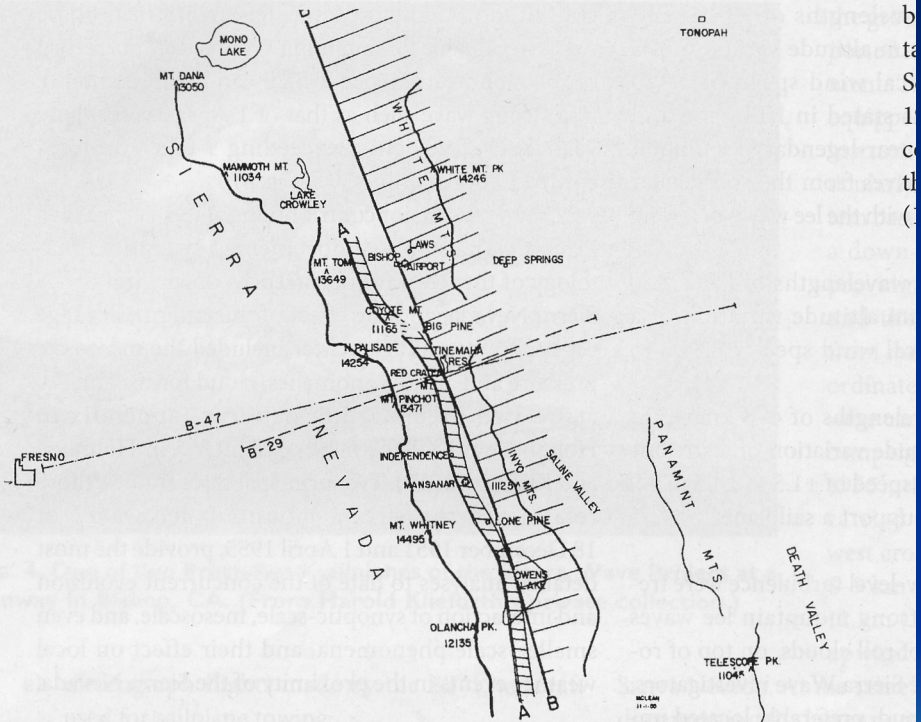

FIG. 6. Typical locations within the Owens Valley of roll clouds associated with normal (AA) and severe (BB) rotors (from Kuettner 1959).

Figure from Grubiši and Lewis (2004)

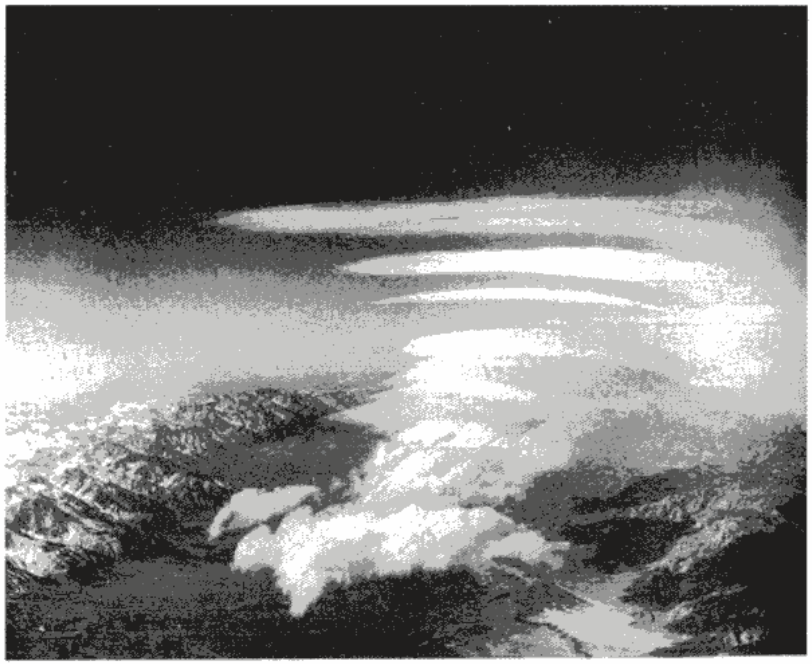

FIG. 7. (top) Clouds at five different levels in a strong mountain wave on 1 Apr 1955 with the roll cloud at approximately 4.5 km, and the highest wave cloud close to 12 km. In the original photo, the view is southward over Owens Valley from 9 km with the Sierra Nevada to the right. Shown is an inverted image of the original photo in which the Sierra Nevada is now to the left. (bottom) A composite display of the B-29 and B-47 measurements of temperature and derived streamline displacements over the Sierra Nevada in a strong mountain wave on 1 Apr 1955 (from Holmboe and Klieforth 1957).

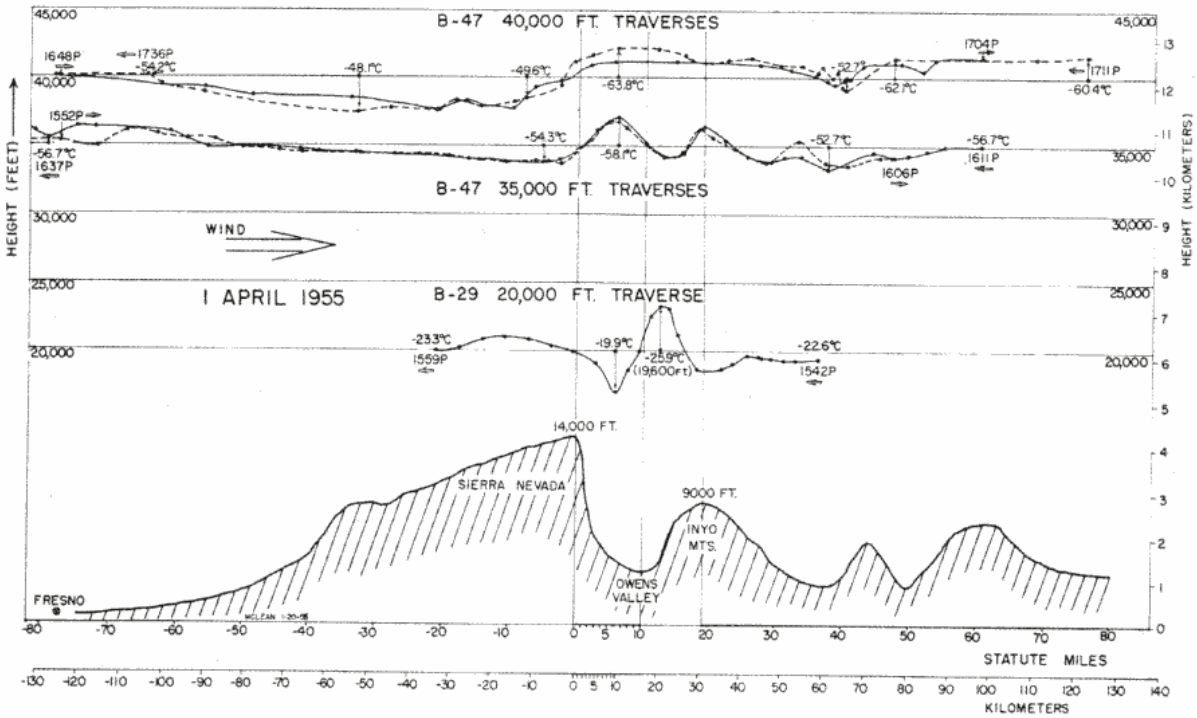

Figure from
Grubiši and Lewis (2004)

Rotor Formation

- Queney (1955) proposed a simple "cat's eye" formation mechanism for rotors
  - Transformation of a stationary wave motion into a system of vortices in the vicinity of a level where the basic wind velocity is vanishing

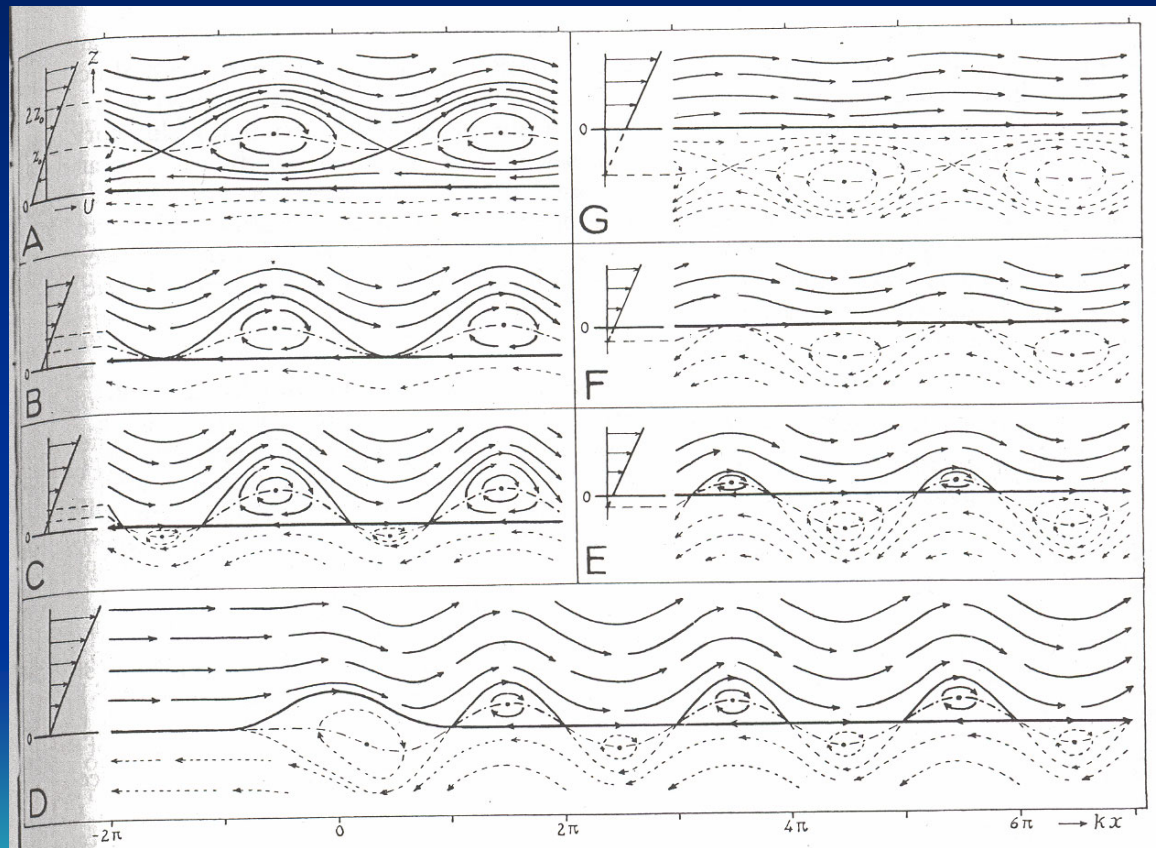

Fig. 1. Stationary wavelike mountain perturbation in a barotropic Couette flow: streamlines corresponding to various wind profiles.

Figure from Queney (1955)

Rotor formation, cont'd

- Doyle and Durran (2002) have a recent paper on rotor dynamics:
  - Kinematic considerations suggest that boundary layer separation is a prerequisite for rotor formation.
  - Numerical simulations suggest that boundary layer separation is greatly facilitated by the adverse pressure gradients associated with trapped mountain lee waves and that boundary layer processes and lee-wave induced pressure gradients interact synergistically to produce low level rotors.
  - Mechanical shear in the planetary boundary layer is the primary source of a sheet of horizontal vorticity that is lifted vertically into the lee wave at the separation point, and partly carried into the rotor.
  - Realistic rotors appear to only develop in the presence of surface friction.
  - Surface heat flux above the lee slope increases the vertical extent of the rotor circulation and the strength of the turbulence but decreases the magnitude of the reversed rotor flow.

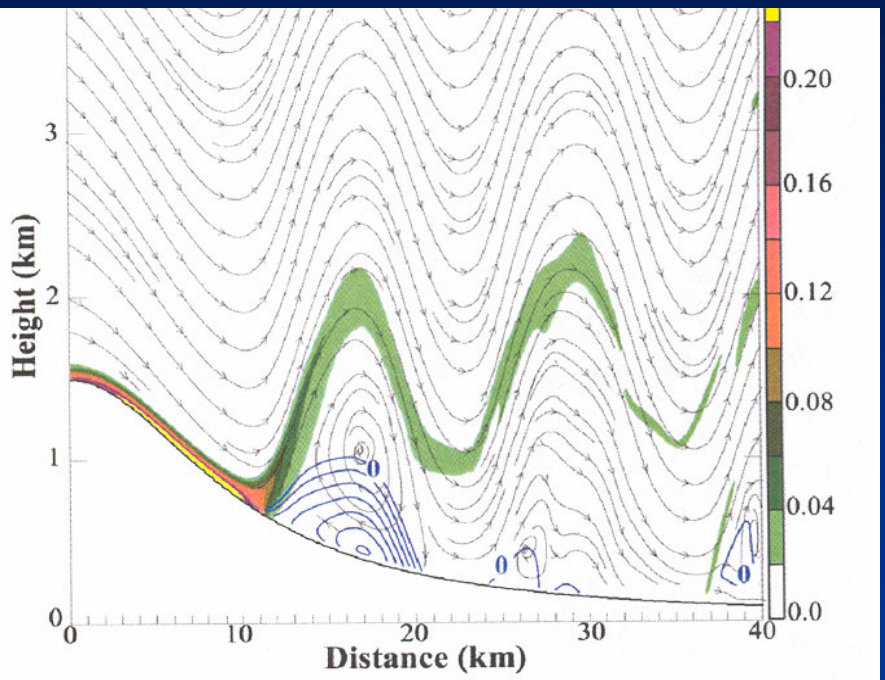

FIG. 3. Streamlines and horizontal vorticity (y-component) from a two-dimensional numerical simulation initialized based on a sounding representative of the conditions in central Colorado at 1200 UTC 3 Mar 1991. The cross-mountain wind speed less than or equal to zero is shown using blue isotachs (every 1 m s^{-1}). The horizontal vorticity greater than 0.02 s^{-1} is shaded in color. (From Doyle and Durran 2002.)

Figure from Doyle and Durran (2004)

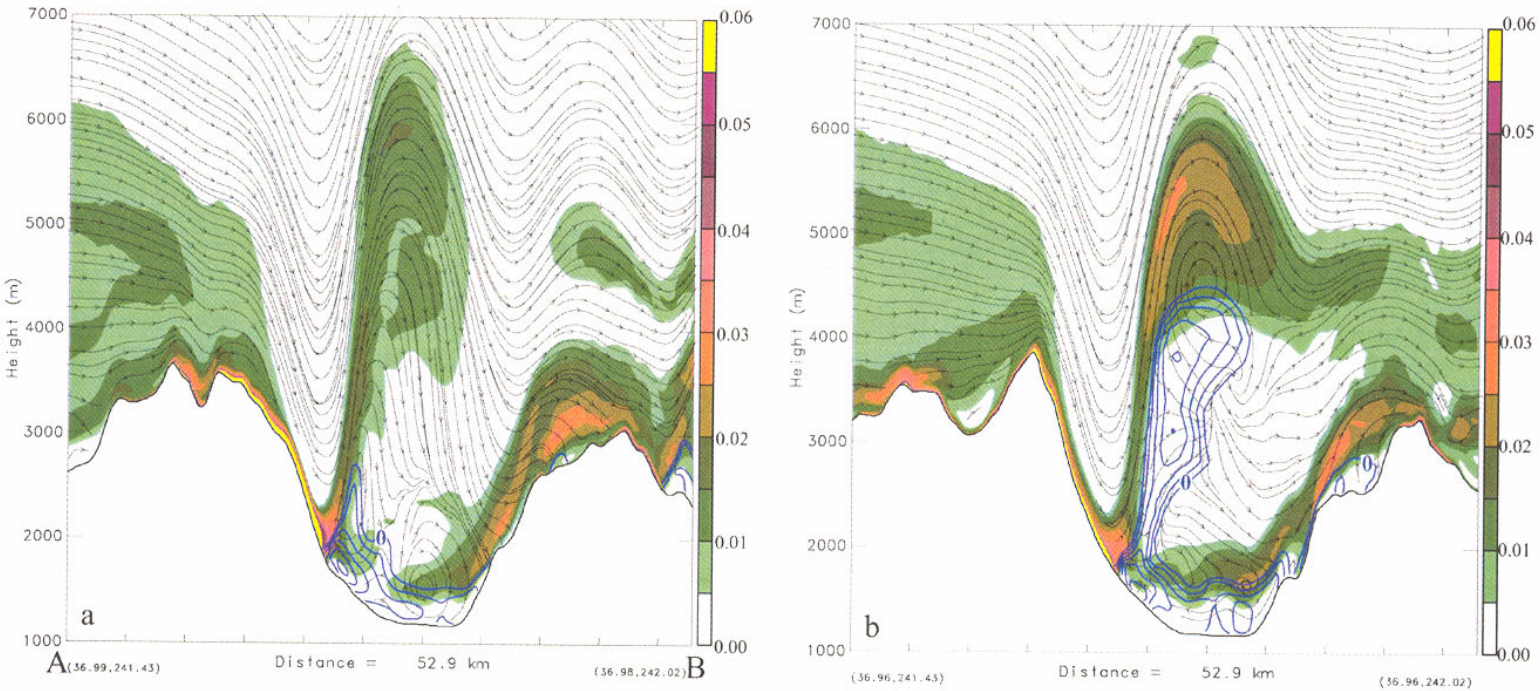

FIG. 7. Streamlines and horizontal vorticity (y-component) from a three-dimensional numerical simulation at the 12-h time valid at 0000 UTC 29 Oct 2000 for (a) along axis AB (see Fig. 6) and (b) approximately 3 km south of axis AB. The horizontal vorticity greater than 0.005 s^{-1} is shaded in color. The cross-mountain wind speed less than or equal to zero is shown using blue isotachs (every 1 m s^{-1}).

Figure from Doyle and Durran (2004)

References

Blier, W., 1998: The Sundowner winds of Santa Barbara, California. *Wea. Forecasting*, **13**, 702--716.

Brinkmann, W. A. R., 1971: What is a foehn? *Weatherwise*, **26**, 230--239.

Brinkmann, W. A. R., 1974: Strong downslope winds at Boulder, Colorado. *Mon. Wea. Rev.*, **102**, 592--602.

Cotton, W. R., J. F. Weaver, and B. A. Beitler, 1995:An unusual summertime downslope wind event in Fort Collins, on 3 July 1993. *Wea. Forecasting*, **10**, 786--797.

Doyle, J. D., and D. R. Durran, 2002: The dynamics of mountain-wave-induced rotors. *J. Atmos. Sci.*, **59**, 186--201.

Doyle, J. D., and D. R. Durran, 2004: Recent developments in the theory of atmospheric rotors. *Bull. Amer. Meteor. Soc.*, **85**, 337--342.

Durran, D. R., 1986a: Another look at downslope windstorms. Part I: The development of analogs to supercritical flow in an infinitely deep, continuously stratified fluid. *J. Atmos. Sci.*, **43**, 2527--2543.

Durran, D. R., 1986b: Mountain waves. *Mesoscale Meteorology and Forecasting*, Ray, P. S., Ed., Amer. Meteor. Soc., 472--492.

Durran, D. R., 1990: Mountain waves and downslope windstorms. *Atmospheric Processes over Complex Terrain*, *Meteor. Monogr.*, No. 45, Amer. Meteor. Soc., 59--81.

Gafn, D. M., 2002: Unexpected warming induced by foehn winds in the lee of the Smoky Mountains. *Wea. Forecasting*, **111**, 907--915.

Glenn, C. L., 1961: The Chinook. *Weatherwise*, **14**, 175--182.

References, Cont'd

Hamann, R. R., 1943: The remarkable temperature fluctuations in the Black Hills region, January 1943. *Mon. Wea. Rev.*, **71**, 29--32.

Hertenstein, R. F., and J. Kuettner, 2002: Simulations of rotors using steep lee-side topography. *10th Conf. on Mountain Meteorology*, Amer. Meteor. Soc., Park City, UT, 330--333.

Hugh D. Cobb, III, 2004: The Gulf of Tehuantepec hurricane force wind event of 30-31 March 2003. *Mar. Wea. Log*, **48**, 7--9.

Jones, C. N., J. D. Colton, R. L. McAnelly, and M. P. Meyers, 2002: An examination of a severe downslope windstorm west of the Colorado Park Range. *Natl. Weather Dig.*, **26**, 73--82.

Julian, L. T., and P. R. Julian, 1969: Boulder's winds. *Weatherwise*, **22**, 108--112, 126.

Klemp, J. B., and D. K. Lilly, 1975: The dynamics of wave-induced downslope winds. *J. Atmos. Sci.*, **32**, 320--339.

Kuettner, J., and R. F. Hertenstein, 2002: Observations of mountain-induced rotors and related hypotheses: A review. *10th Conf. on Mountain Meteorology*, Amer. Meteor. Soc., Park City, UT, 326--329.

Kuettner, J. P., 1968: Lee waves in the Colorado Rockies. *Weatherwise*, **21**, 180--185, 193, 197.

Lee, T. J., R. A. Pielke, R. C. Keesler, and J. Weaver, 1989: Influence of cold pools downstream of mountain barriers on downslope winds and flushing. *Mon. Wea. Rev.*, **117**, 2041--2058.

Lessard, A. G., 1988: The Santa Ana winds of southern California. *Weatherwise*, **41**, 100--104.

References, Cont'd

Lilly, D. K., 1978: A severe downslope windstorm and aircraft turbulence event induced by a mountain wave. *J. Atmos. Sci.*, **35**, 59--77.

Lilly, D. K., and E. J. Zipser, 1972: The Front Range windstorm of 11 January 1972. A meteorological narrative. *Weatherwise*, 56--63.

Long, R. R., 1953a: Some aspects of the flow of stratified fluids. I. A theoretical investigation. *Tellus*, **5**, 42--58.

Long, R. R., 1953b: Steady motion around a symmetrical obstacle moving along the axis of a rotating fluid. *J. Meteor.*, **10**, 197--203.

Long, R. R., 1954: Some aspects of the flow of stratified fluids. II. Experiments with a two fluid system. *Tellus*, **6**, 97--115.

Long, R. R., 1955: Some aspects of the flow of stratified fluids. III. Continuous density gradients. *Tellus*, **7**, 341--357.

Manley, G., 1945: The Helm Wind of Crossfell, 1937-1939. *Quart. J. Roy. Meteor. Soc.*, **71**, 197--219.

Meyers, M. P., J. S. Snook, D. A. Wesley, and G. S. Poulos, 2003: A Rocky Mountain storm. Part II: The forest blowdown over the West Slope of the northern Colorado mountains--Observations, analysis, and modeling. *Wea. Forecasting*, **18**, 662--674.

Peltier, W. R., and J. F. Scinocca, 1990: The origin of severe downslope windstorm pulsations. *J. Atmos. Sci.*, **47**, 2853--2870.

Pirazzoli, P. A., and A. Tomasin, 1999: Recent abatement of easterly winds in the northern Adriatic. *Int. J. Climatol.*, **19**, 1205--1219.

Queney, P., 1955: Rotor phenomena in the lee of mountains. *Tellus*, **7**, 367--371.

References, Cont'd

Raphael, M. N., 2003: The Santa Ana winds of California. *Earth Interactions*, **7**, 1--13.

Riehl, H., 1971: An unusual Chinook case. *Weather*, **26**, 241--246.

Rotunno, R., and P. K. Smolarkiewicz, 1995: Vorticity generation in the shallow-water equations as applied to hydraulic jumps. *J. Atmos. Sci.*, **52**, 320--330.

Scorer, R. S., 1949: Theory of waves in the lee of mountains. *Quart. J. Roy. Meteor. Soc.*, **75**, 41--56.

Scorer, R. S., and H. Klieforth, 1958: Theory of mountain waves of large amplitude. *Quart. J. Roy. Meteor. Soc.*, **84**, 131--142.

Smith, R. B., 1979: The influence of mountains on the atmosphere. *Advances in Geophysics*, Saltzman, B., Ed., Vol. 21, Academic Press, 87--230.

Smith, R. B., 1985: On severe downslope winds. *J. Atmos. Sci.*, **42**, 2597--2603.

Grubiši, V. and J. M. Lewis, 2004: Sierra Wave Project Revisited: 50 Years Later. *Bulletin of the American Meteorological Society,* **85**, 1127–1142.

Weaver, J. F., and R. S. Phillips, 1990: An expert system application for forecasting severe downslope winds at Fort Collins, Colorado, U.S.A. *16th Conf. on Severe Local Storms*, Amer. Meteor. Soc., Kananaskis Park, AB, Canada, 13--15.

Whiteman, C. D., 2000: Terrain-forced flows. *Mountain Meteorology: Fundamentals and Applications*, Oxford Univ. Press, 141--170.

Whiteman, C. D., and J. G. Whiteman, 1973: An historical climatology of damaging downslope windstorms at Boulder, Colorado. NOAA Technical Report ERL 336-APCL 35, NOAA/ERL, Boulder, Colo. 62 pp.

Wolyn, P. G., 2003: Mountain-wave induced windstorms west of Westcliffe, Colorado. *10th Conf. on Mountain Meteorology*, Amer. Meteor. Soc., Park City, UT, 402--405.

Yoshino, M. M., 1971: Die bora in jugoslawien: Eine synoptischeklimatologische betrachtung. *Ann. Meteor.*, **5**, 117--121.